Electronic Supplementary Material (ESI) for New Journal of Chemistry.

Medium sized cyclic bis(anisylphosphonothioyl) disulfanes and the corresponding related cyclic sulfanes - structure and the most characteristic reactions

Witold Przychodzeń*, Jarosław Chojnacki, Łukasz Nierzwicki

Faculty of Chemistry, Gdańsk University of Technology, Narutowicza 11, 80233 Gdansk (Poland) E-mail: witold.przychodzen@pg.edu.pl

Electronic Supplementary Information

Materials

Merck silica gel (particle size 0.04–0.063 mm) was used for conventional silica gel chromatography, while thin-layer chromatography was performed using Merck silica-gel 60 F254 coated on aluminium sheets. THF was distilled from potassium-benzophenone ketyl. Lawesson's reagent (Sigma-Aldrich) was recrystallized from chlorobenzene prior to use. Ethylene glycol, neopentyl glycol, 1,4-butanediol, 1,6-hexanediol and 2-chloro-*N*-methylpyridinium iodide (Mukaiyama's reagent MR) were commercially available (Sigma-Aldrich) and were used as received. Ethyl 3-hydroxy-2-(hydroxymethyl)propanoate was prepared according to a reported procedure.[1] Cyclic disulfanes **2a, 2b** and **2c** were obtained using the previously described procedure [8, 12] and acyclic **2h** according to Grossmann's procedure [22].

Instrumentation

NMR spectra were recorded on a Varian Unity Inova 500 MHz and on a Bruker AVANCE 400 MHz spectrometers with TMS or H_3PO_4 as external standards. ^{1}H and ^{13}C spectra were obtained in $CDCl_3$ and ^{31}P NMR spectra in $CDCl_3$ or $MeCN/C_6D_6$ 10:1 (v/v) solutions. The assignment of the chemical shifts and coupling constants of the complex spin systems formed by the OCH_2 protons in cyclic disulfanes **2** and sulfanes **3** was made by ^{1}H,^{1}H-COSY and decoupled ^{31}P and/or ^{1}H NMR experiments. The couplings $^nJ_{PC}$ observed as deceptive triplets or quintets, indicating the second-order effects, were described as multiplets (m) and their values were estimated by measuring the distances between the external transitions of the respective multiplets. IR spectra were recorded on a Thermo Scientific Nicolet 6700 spectrometer outfitted with a Smart Orbit diamond ATR cell or on a FTIR spectrometer (ATR method; NICOLET iS5; Thermo Fisher Scientific, Waltham, MA, USA) at wavenumbers of 400 to 4000 cm^{-1}. Powder samples of pure analyte were pressed onto the cell window. Raman spectra of crystals were recorded with an Aramis Horiba Jobin-Yvon micro-Raman spectrometer, using a solid state 500 mW visible laser operating at 532 nm. MS/MS positive ion mode mass spectra (70-120 V) were obtained using a 4000 Q TRAP hybrid triple quadrupole linear ion trap mass spectrometer (Applied Biosystems/MDS Sciex).

X-ray analyses were carried out using KUMA KM4 CCD (6 cases) or Stoe IPDS instruments (4 cases, see Supp. Info.). KUMA: Diffraction data were recorded at 120.0 (2) K or at room temperature 293.0 (2) K on a KUMA KM4 (Wrocław, Poland) diffractometer with graphite-monochromated Mo Ka radiation (0.71073 Å), equipped with a Sapphire 2 CCD camera (Oxford Diffraction, Yarnton, England). Data collection was performed using CrysAlisPro (Agilent Technologies, 2013) in the ω-scan mode. Analytical absorption correction was applied for all strongly absorbing crystals.

Stoe: Diffraction intensity data were collected on an IPDS 2T dual-beam diffractometer (Stoe & Cie GmbH, Darmstadt, Germany) at 120.0 (2) K with Mo Kα radiation of a microfocus X-ray source (GeniX 3D Mo High Flux, Xenocs, Sassenage, 50 kV, 1.0 mA, λ = 0.71069 Å). The crystal was thermostated in a nitrogen stream at 120 K using a Cryo-Stream-800 device

[1] S. Yoshida, K. Obitsu, Y. Hayashi, M. Shibazaki, T. Kimura,T. Takahashi, T. Asano, H. Kubota, and T. Mukuta, *Org. Process Res. Dev*., 2012, **16**, 1527−1537.

(Oxford CryoSystem, UK) during the entire experiment. Data collection and reduction were controlled by X-Area_1.75 (Stoe, 2015). An absorption correction was performed on the integrated reflections by a combination of frame scaling, reflection scaling and a spherical absorption correction. Outliers have been rejected according to Blessing's method (Blessing, 1997).

Characterization data for compounds 2b, 2b', 2d, 3a-3c and 4a

8-Ethoxycarbonyl-2,5-*bis*(4-methoxyphenyl)-8-methyl-1,6,3,4,2,5-dioxadithiadiphosphonane 2,5-disulfide (2b'). Yield: 0.468 g (85%); mp 112 °C (from ethyl acetate-cyclohexane). NMR (δ in ppm): ^{1}H NMR ($CDCl_3$) 1.32 (t, 3H, CH_3), 3.29 (m, 1H, C2H), 3.87 and 3.88 (2 x s, OCH_3), 4.29 (m, 2H, OCH_2CH_3), 4.49 (ddd, $^2J_{HH}$ = 10.2 Hz, $^3J_{HH}$ = 5.3 Hz, $^3J_{HP}$ = 1.5 Hz, 1H, C1/3H_{eq1}), 4.66 (ddd, $^2J_{HH}$ = 10.2 Hz, $^3J_{HH}$ = 2.0 Hz $^3J_{HP}$ = 1.5 Hz, 1H, C1/3H_{eq2}), 4.82 (ddd, $^2J_{HH}$ = 10.2 Hz, $^3J_{PH}$ = 7.1 Hz, $^3J_{HH}$ = 3.0 Hz, 1H, C1/3H_{ax1}), 4.85 (ddd, $^2J_{HH}$ = 10.2 Hz, $^3J_{PH}$ = 7.1 Hz, $^3J_{HH}$ = 1.0 Hz, 1H, C1/3H_{ax2}), 7.01 (dd, $^3J_{HH}$ = 8.8 Hz, $^4J_{HP}$ = 3.9 Hz, 2H, C3'/5'), 7.02 (dd, $^3J_{HH}$ = 8.8 Hz, $^4J_{HP}$ = 3.9 Hz, 2H, C3'/5'), 7.87 (dd, $^3J_{HP}$ = 13.7 Hz, $^3J_{HH}$ = 8.8 Hz, 2H, C2'/6'), 7.91 (dd, $^3J_{HP}$ = 13.7 Hz, $^3J_{HH}$ = 8.8 Hz, 2H, C2'/6'); ^{13}C NMR ($CDCl_3$) 14.44 (CH_3), 44.48 (t, $^3J_{CP}$ = 10.1 Hz, CH), 55.79 and 55.80 (OCH_3), 60.62 (d, $^2J_{CP}$ = 4.3 Hz, $POCH_2$), 62.03 ($COOCH_2$), 114.43 (d, J = 16.7 Hz, C3'/5'), 114.46 (d, J = 16.8 Hz, C3''/5''), 124.03 (d, J_1 = 134 Hz, C1'), 124.09 (d, J_1 = 134 Hz, C1''), 133.40 (d, J = 13.4 Hz, C2'/6'), 133.42 (d, J = 13.5 Hz, C2''/6''), 163.72 (C4'), 163.75 (C4''), 169.23 (C=O); ^{31}P{^{1}H}NMR ($CDCl_3$) 88.9 ($^3J_{PP}$ = 4.2 Hz), 89.9 ($^3J_{PP}$ = 4.2 Hz); ^{31}P NMR (nodec): 88.9 (tddtd, $^3J_{PHaryl}$ = 14.1 Hz, $^3J_{PHalkyl}$ = 13.3Hz, $^3J_{PP}$ = 4.2 Hz, $^4J_{PHaryl}$ = 3.9 Hz, $^3J_{PHalkyl}$ = 1.5 Hz) 89.9 (tddtd, $^3J_{PHaryl}$ = 14.1 Hz, $^3J_{PHalkyl}$ = 13.3 Hz, $^3J_{PP}$ = 4.2 Hz, $^4J_{PHaryl}$ = 3.9 Hz, $^3J_{PHalkyl}$ = 1.5 Hz). MS calcd for $[C_{20}H_{24}O_6P_2S_4]^+$ $(M)^+$: 549.99; found: 551.1 $[M+H]^+$.

2,5-*bis*(4-methoxyphenyl)-1,6,3,4,2,5-dioxadithiadiphosphacyclododecane 2,5-disulfide (2d). Yield: 0.094 g (18%); mp 157-159 °C (from chloroform-cyclohexane). NMR (δ in ppm): ^{1}H NMR ($CDCl_3$) 1.67 (m, 4H), 1.82 (m, 2H), 2.09 (m, 2H), 3.84 (s, 6H, OCH_3), 4.27 (dddd, $^3J_{HH}$ = 11.6 Hz, $^2J_{HH}$ = 10.0 Hz, $^3J_{HP}$ = 5.4 Hz, $^3J_{HH}$ = 2.2 Hz, 2H, H_A, 2H), 4.49 (ddt, $^2J_{HH}$ = 10.0 Hz, $^3J_{HP}$ = 9.3 Hz, $^3J_{HH}$ = 3.5 Hz, 2H, H_B), 7.01 (dd, $^3J_{HH}$ = 8.8 Hz, $^4J_{HP}$ = 3.9 Hz, 4H), 7.83 (dd, $^3J_{HP}$ = 13.7 Hz, $^3J_{HH}$ = 8.8 Hz, 4H); ^{13}C NMR ($CDCl_3$): 21.42 (C3), 28.59 (d, J = 11.4 Hz, C2), 55.76 (C-7'), 63.79 (m, J = 4.8 Hz, C1), 114.47 (d, J = 17.6 Hz, C-3'/5'), 124.52 (d, J = 134 Hz, C-1'), 133.33 (d, J = 14.5 Hz, C-2'/6'), 163.49 (C-4'); ^{31}P{^{1}H} NMR ($CDCl_3$): 89.99 ($^3J_{PP}$ = 4 Hz). Calc. for $C_{20}H_{26}O_4P_2S_4$: 520.02. Found: 521.0 $[M+H]^+$.

cis-**2,4-*bis*(4-methoxyphenyl)-1,5,3,2,4-dioxathiadiphosphepane 2,4-disulfide** (*cis*-**3a**). Yield: 0.039 g (9%); colourless needles; mp 133-134 °C (from ethyl acetate-hexane); R_f = 0.06 (chloroform-hexane 1:1), R_f = 0.29 (hexane-ethyl acetate 7:3). NMR (δ in ppm): ^{1}H NMR ($CDCl_3$) 3.83 (s, 6H, OCH_3), 4.48 (m, 2H), 5.17 (m, 2H), 6.79 (dd, $^3J_{HH}$ = 8.8 Hz, $^4J_{HP}$= 3.4 Hz, 4H), 7.62 (dd, $^3J_{HP}$ = 14.7 Hz, $^3J_{HH}$ = 8.8 Hz, 4H); ^{13}C NMR ($CDCl_3$) 55.49 (CH_3O), 65.18 (d, $^2J_{CP}$ = 7 Hz, OCH_2), 113.84 (d, $^3J_{CP}$ = 17.0 Hz, C-3'/5'), 126.62 (d, $^1J_{CP}$ = 135 Hz, C-1'), 132.69 (m, $^2J_{CP}$ = 14.5 Hz, C2'/6'), 163.09 (d, $^4J_{CP}$ = 3.4 Hz, C-4'); ^{31}P{^{1}H} NMR ($MeCN-CH_2Cl_2$ 1:1, 10% C_6D_6) 85.92. Calc. for $C_{16}H_{18}O_4P_2S_3$: 431.98. Found: 433.0 $[M+H]^+$.

trans-**2,4-*bis*(4-methoxyphenyl)-[1,5,3,2,4-dioxathiadiphosphepane 2,4-disulfide** (*trans*-**3a**). Yield: 0.329 g (76%); colourless needles; mp 129-130 °C (from ethyl acetate-hexane); R_f = 0.15 (chloroform-hexane 1:1), R_f = 0.53 (hexane-ethyl acetate 7:3); NMR (δ in ppm): ^{1}H NMR ($CDCl_3$) 3.86 (s, 6H, OCH_3), 4.32 (m, 2H), 5.23 (m, 2H), 6.99 (dd, $^3J_{HH}$ = 8.8 Hz, $^4J_{HP}$= 3.4 Hz, 4H), 8.13 (dd, $^3J_{HP}$ = 14.7 Hz, $^3J_{HH}$ = 8.8 Hz, 4H); ^{13}C NMR ($CDCl_3$) 55.77

(CH_3O), 66.38 (m, $^2J_{CP}$ = 7.0 Hz, OCH_2), 114.12 (m, $^3J_{CP}$ = 16.8 Hz, C-3'/5'), 125.85 (d, $^1J_{CP}$ = 136.1 Hz, C-1'), 133.88 (m, $^2J_{CP}$ = 14.2 Hz, C2'/6'), 163.69 (s, C-4'); $^{31}P\{^1H\}$ NMR (MeCN-CH_2Cl_2 1:1, 10% C_6D_6): 89.04 ($^2J_{PP}$ = -13 Hz). Calc. for $C_{16}H_{18}O_4P_2S_3$: 431.98. Found: 433.0 $[M+H]^+$.

cis-**2,4-*bis*(4-methoxyphenyl)-7,7-dimethyl-1,5,3,2,4-dioxathiadiphosphocane 2,4-disulfide** (*cis*-**3b**). Yield: 0.186 g (43%); colourless prisms; mp 196-198 °C (from ethyl acetate-cyclohexane); R_f = 0.50 (hexane-ethyl acetate 7:3). NMR (δ in ppm): ^1H NMR ($CDCl_3$) 1.01 and 1.41 (2 x s, 6H, CH_3C), 3.76 (s, 6H, OCH_3), 3.83 (dd, $^2J_{HH}$ = 10.7 Hz, $^3J_{HP}$ = 7.3 Hz, 2H, H_A), 4.52 (dd, $^2J_{HH}$ = 10.7 Hz, $^3J_{HP}$ = 18.6 Hz, 2H, H_B), 6.53 (dd, $^3J_{HH}$ = 8.8 Hz, $^4J_{HP}$ = 3.0 Hz, 4H), 7.34 (dd, $^3J_{HP}$ = 14.1 Hz, $^3J_{HH}$ = 8.8 Hz, 4H); ^1H NMR (C_6D_6) 0.13 and 0.95 (2 x s, 6H, CH_3C), 3.07 (s, 6H, OCH_3), 3.32 (dd, $^2J_{HH}$ = 10.9 Hz, $^3J_{HP}$ = 7.5 Hz, 2H, H_A), 4.56 (dd, $^2J_{HH}$ = 11.0 Hz, $^3J_{HP}$ = 18.8 Hz, 2H, H_B), 6.09 (dd, $^3J_{HH}$ = 8.7 Hz, $^4J_{HP}$ = 3.0 Hz, 4H), 7.31 (dd, $^3J_{HP}$ = 14.0 Hz, $^3J_{HH}$ = 8.7 Hz, 4H); ^{13}C NMR ($CDCl_3$) 21.68 and 21.79 (2 x s, CH_3), 36.18 (m, $^3J_{CP}$ = 9.6 Hz, *C*CH_3), 55.37 (s, CH_3O), 74.02 (m, $^2J_{CP}$ = 6.7 Hz, OCH_2), 113.88 (m, $^3J_{CP}$ = 16.8 Hz, C-3'/5'), 124.89 (d, $^1J_{CP}$ = 139.7 Hz, C-1'), 132.18 (m, $^2J_{CP}$ = 13.8 Hz, C2'/6'), 162.65 (m, $^4J_{CP}$ = 3.5 Hz, C-4'); $^{31}P\{^1H\}$ NMR (MeCN-CH_2Cl_2 1:1, 10% C_6D_6) 86.09. Calc. for $C_{19}H_{24}O_4P_2S_3$: 474.03. Found: 475.1 $[M+H]^+$.

trans-**2,4-*bis*(4-methoxyphenyl)-7,7-dimethyl-1,5,3,2,4-dioxathiadiphosphocane 2,4-disulfide** (*trans*-**3b**). Yield: 0.242 g (51%); colourless needles; mp 161-163 °C (from ethyl acetate-hexanes); R_f = 0.58 (hexane-ethyl acetate 7:3). NMR (δ in ppm): ^1H NMR ($CDCl_3$) 1.17 (s, 6H, CCH_3), 3.74 (dd, $^2J_{HH}$ = 11.0, $^3J_{HP}$ = 8.0 Hz, 2H), 3.87 (s, 6H, OCH_3), 4.74 (dd, $^2J_{HH}$ = 11.0 Hz, $^3J_{HP}$ = 18.0 Hz, 2H), 6.98 (dd, $^3J_{HH}$ = 8.8 Hz, $^4J_{HP}$ = 2.9 Hz, 4H), 7.93 (dd, $^3J_{HP}$ = 14.1 Hz, $^3J_{HH}$ = 8.8 Hz, 4H, ArH); ^1H NMR (C_6D_6) 0.64 (s, 6H, CCH_3), 3.05 (s, 6H, OCH_3), 3.37 (dd, $^2J_{HH}$ = 10.8, $^3J_{HP}$ = 7.3 Hz, 2H), 4.76 (dd, $^2J_{HH}$ = 10.8 Hz, $^3J_{HP}$ = 17.5 Hz, 2H), 6.61 (dd, $^3J_{HH}$ = 8.8 Hz, $^4J_{HP}$ = 3.0 Hz, 4H), 8.07 (dd, $^3J_{HP}$ = 13.9 Hz, $^3J_{HH}$ = 8.7 Hz, 4H, ArH); ^{13}C NMR ($CDCl_3$) 22.37 (s, CH_3), 36.24 (m, $^3J_{CP}$ = 10.5 Hz, *C*CH_3), 55.72 (s, C-7'), 71.82 (m, $^2J_{CP}$ = 6.4 Hz, OCH_2), 114.05 (m, $^3J_{CP}$ = 16.8 Hz, C-3'/5'), 125.35 (d, $^1J_{CP}$ = 136 Hz, C-1'), 133.34 (m, $^2J_{CP}$ = 14.0 Hz, C2'/6'), 163.47 (m, $^4J_{CP}$ = 3.5 Hz, C-4'); $^{31}P\{^1H\}$ NMR (MeCN-CH_2Cl_2 1:1, 10% C_6D_6) 87.70. Calc. for $C_{19}H_{24}O_4P_2S_3$: 474.03. Found: 475.1 $[M+H]^+$.

cis-**2,4-*bis*(4-methoxyphenyl)-1,5,3,2,4-dioxathiadiphosphonane 2,4-disulfide** (*cis*-**3c**). Yield: 0.170 g (37%); colourless prisms; mp 197-199 °C (from benzene-cyclohexane); R_f = 0.52 (hexane-ethyl acetate 7:3). NMR (δ in ppm): ^1H NMR ($CDCl_3$) 2.17 (m, 2H, CH_2), 2.27 (m, 2H, CH_2), 3.76 (s, 6H, OCH_3), 4.21 (m, 2H, OCH_2), 4.91 (m, 2H, OCH_2), 6.55 (dd, $^3J_{HH}$ = 8.8 Hz, $^4J_{HP}$ = 3.5 Hz, 4H, ArH), 7.37 (dd, $^3J_{HP}$ = 14.2 Hz, $^3J_{HH}$ = 8.8 Hz, 4H, ArH); ^{13}C NMR ($CDCl_3$) 27.90 (m, $^3J_{CP}$ = 4.4 Hz, *C*H_2CH_2O), 55.15 (s, CH_3O), 67.38 (m, $^2J_{CP}$ = 7.2 Hz, OCH_2), 113.55 (m, $^3J_{CP}$ = 16.9 Hz, C-3'/5'), 125.61 (m, $^1J_{CP}$ = 137.4 Hz, C-1'), 132.06 (m, $^2J_{CP}$ = 14.0 Hz, C2'/6'), 162.27 (m, $^4J_{CP}$ = 3.7 Hz, C-4'); $^{31}P\{^1H\}$ NMR (MeCN-CH_2Cl_2 1:1, 10% C_6D_6) 85.6 ($^2J_{PP}$ = -21 Hz). Calc. for $C_{18}H_{22}O_4P_2S_3$: 460.02. Found: 461.1 $[M+H]^+$.

trans-**2,4-*bis*(4-methoxyphenyl)-1,5,3,2,4-dioxathiadiphosphonane 2,4-disulfide** (*trans*-**3c**). Yield: 0.110 g (24%); colourless needles; mp 171-172 °C (from ethyl acetate-cyclohexane); R_f = 0.57 (hexane-ethyl acetate 7:3). NMR (δ in ppm): ^1H NMR ($CDCl_3$) 2.06 (m, 2H, CH_2), 2.22 (m, 2H, CH_2), 3.86 (s, 6H, OCH_3), 4.20 (m, 2H, OCH_2), 4.95 (m, 2H, OCH_2), 6.96 (dd, $^3J_{HH}$ = 8.8 Hz, $^4J_{HP}$ = 3.5 Hz, 4H, ArH), 7.89 (dd, $^3J_{HP}$ = 14.2 Hz, $^3J_{HH}$ = 8.8 Hz, 4H, ArH); ^{13}C NMR ($CDCl_3$) 27.36 (m, $^3J_{PC}$ = 5.3 Hz, *C*H_2CH_3), 55.69 (s, CH_3O), 68.09 (m, $^2J_{CP}$ = 7.1 Hz, OCH_2), 114.05 (m, $^3J_{CP}$ = 16.8 Hz, C-3'/5'), 127.66 (d, $^1J_{CP}$ = 135.2 Hz, C-1'), 133.08 (m, $^2J_{CP}$ = 14.1 Hz, C2'/6'), 163.24 (s, C-4'); $^{31}P\{^1H\}$ NMR (MeCN-CH_2Cl_2 1:1, 10% C_6D_6) 86.5 ($^2J_{PP}$ = -14 Hz). Calc. for $C_{18}H_{22}O_4P_2S_3$: 460.02. Found: 461.1 $[M+H]^+$.

2-(4-methoxyphenyl)-1,3,2-dioxaphospholane 2-sulfide (4a) (Method B). Yield: 0.075 g (30%); colourless prisms; mp 84-85 ^{o}C (from ethyl acetate-cyclohexane, lit. [14] m.p 76 ^{o}C); R_f = 0.27 (hexane-ethyl acetate 7:3). NMR (δ in ppm): ^{1}H NMR ($CDCl_3$) 3.89 (s, 3H, OCH_3), 4.43 (m, 2H, OCH_2), 4.62 (m, 2H, OCH_2), 6.99 (dd, $^{3}J_{HH}$ = 8.8 Hz, $^{4}J_{HP}$ = 3.4 Hz, 4H, ArH), 7.85 (dd, $^{3}J_{HP}$ = 14.3 Hz, $^{3}J_{HH}$ = 8.8 Hz, 4H, ArH); ^{13}C NMR ($CDCl_3$) 55.32 (s, CH_3O), 66.77 (d, $^{2}J_{CP}$ = 7.1 Hz, OCH_2), 113.82 (d, $^{3}J_{CP}$ = 16.5 Hz, C-3'/5'), 123.97 (d, $^{1}J_{CP}$ = 145.0 Hz, C-1'), 133.28 (d, $^{2}J_{CP}$ = 14.4 Hz, C2'/6'), 163.26 (d, $^{4}J_{CP}$ = 3.3 Hz, C-4'); ^{31}P NMR ($CDCl_3$) 106.5 (tddd, $^{3}J_{PH}$ = 23.4, $^{3}J_{PH'}$ = 14.3, $^{4}J_{PH'}$ = 3.4, $^{3}J_{PH}$ = 1.4 Hz).

NMR Spectra and NMR spectral parameters of Compounds 2 - 4

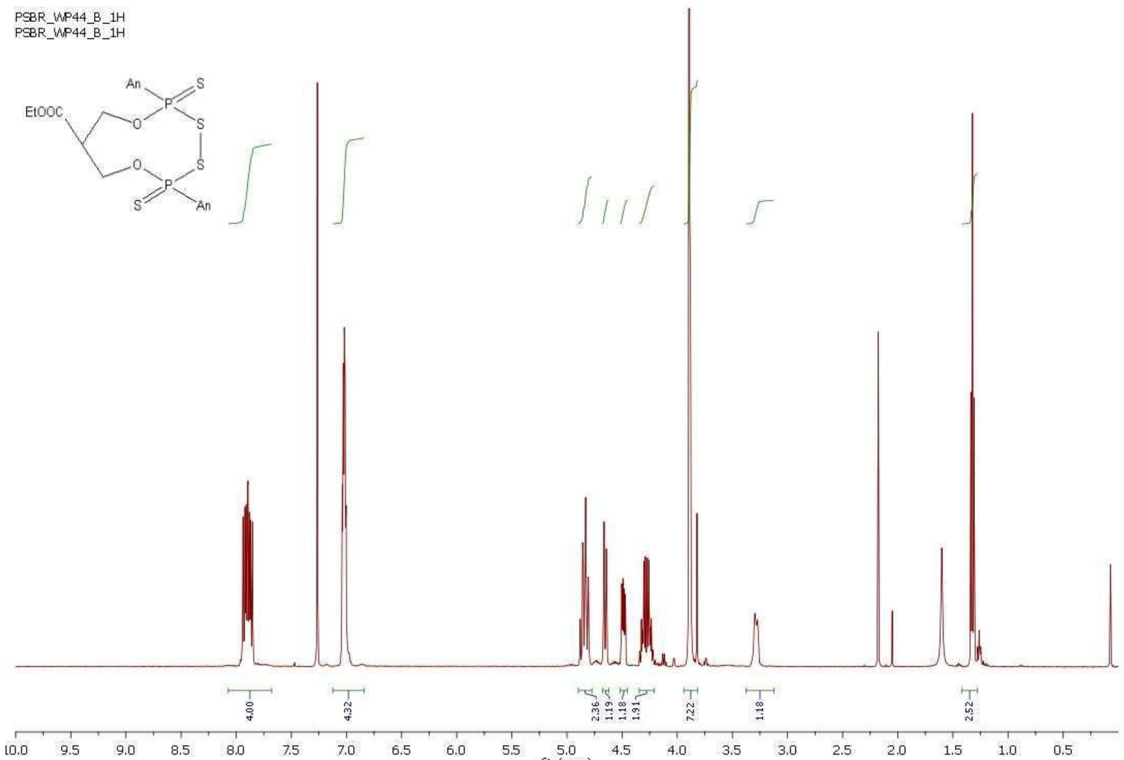

Figure S1. ^{1}H NMR spectrum of **2b'** in $CDCl_3$

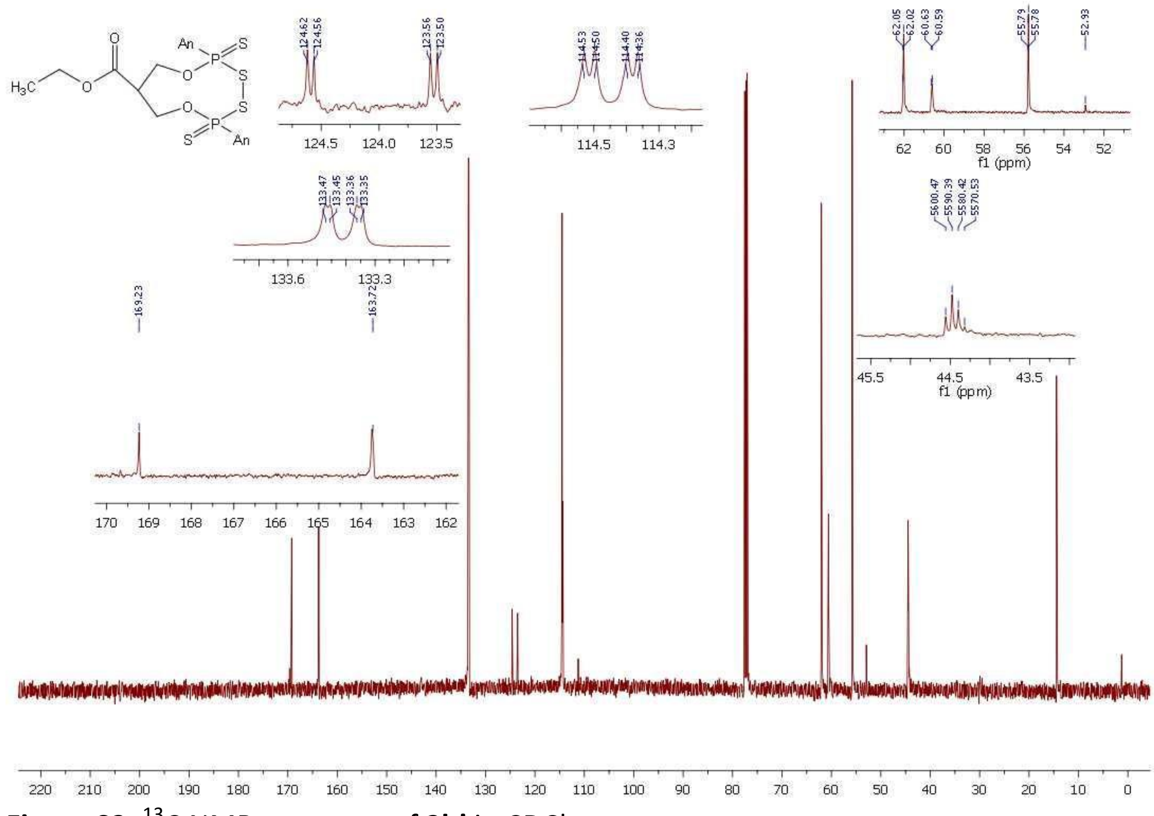

Figure S2. ^{13}C NMR spectrum of **2b'** in $CDCl_3$

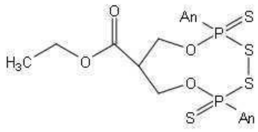

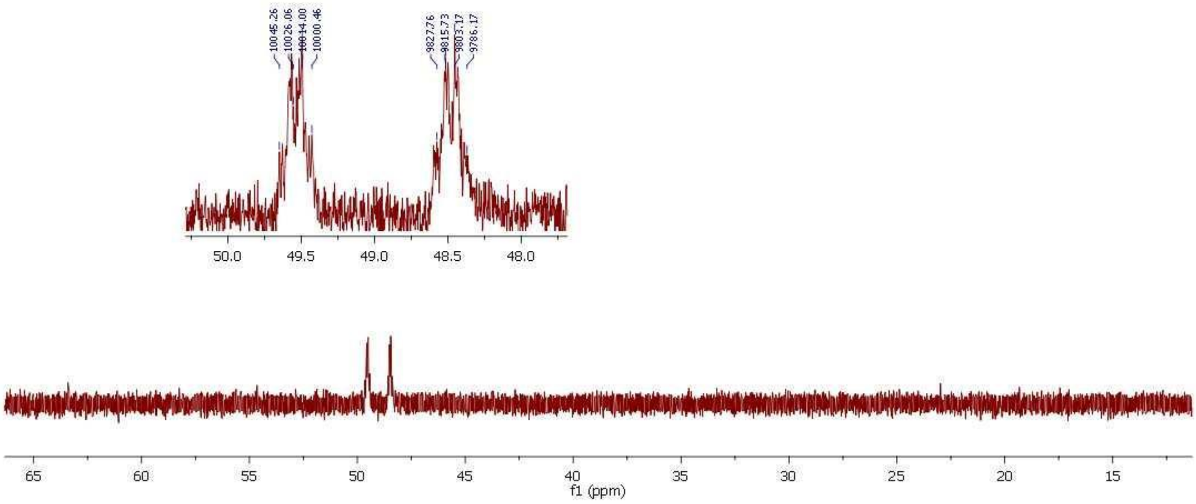

Figure S3. $^{31}P\ \{^{1}H\}$ NMR spectrum of **2b'** in $CDCl_3$

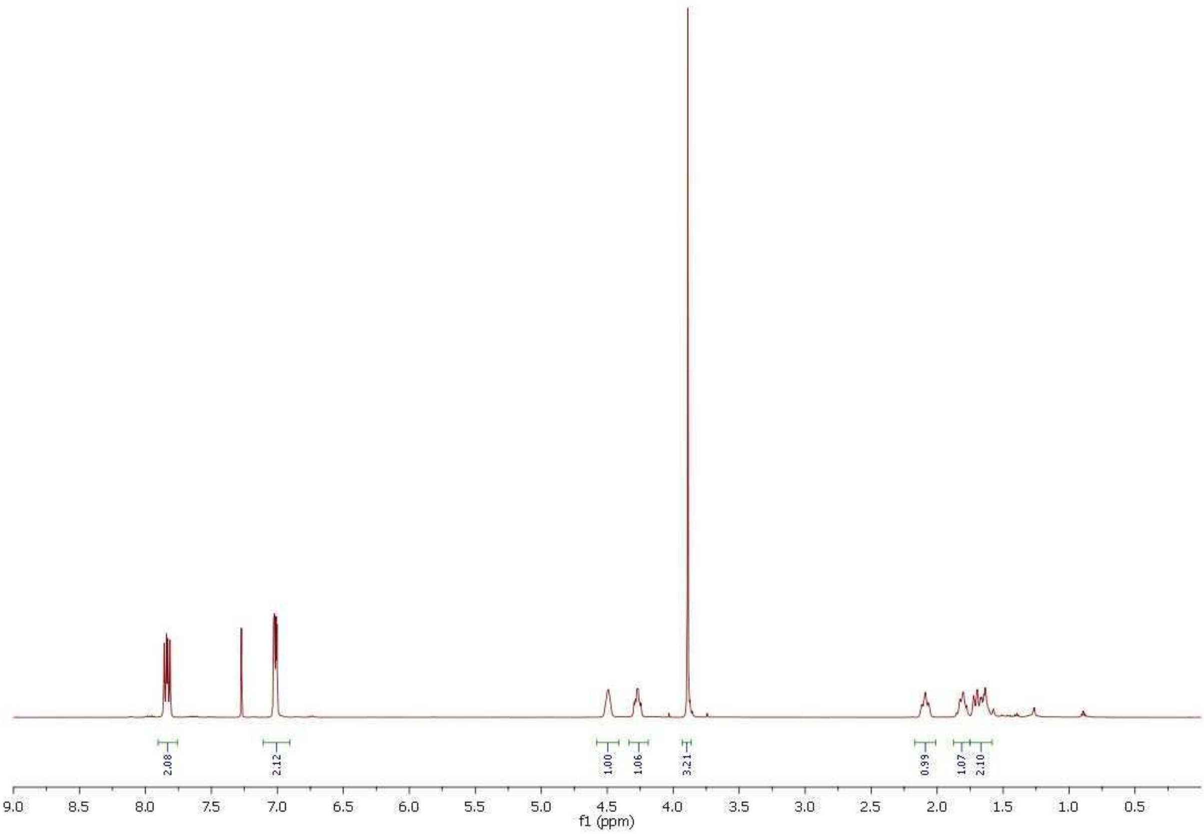

Figure S4. ^{1}H NMR spectrum of **2d** in $CDCl_3$

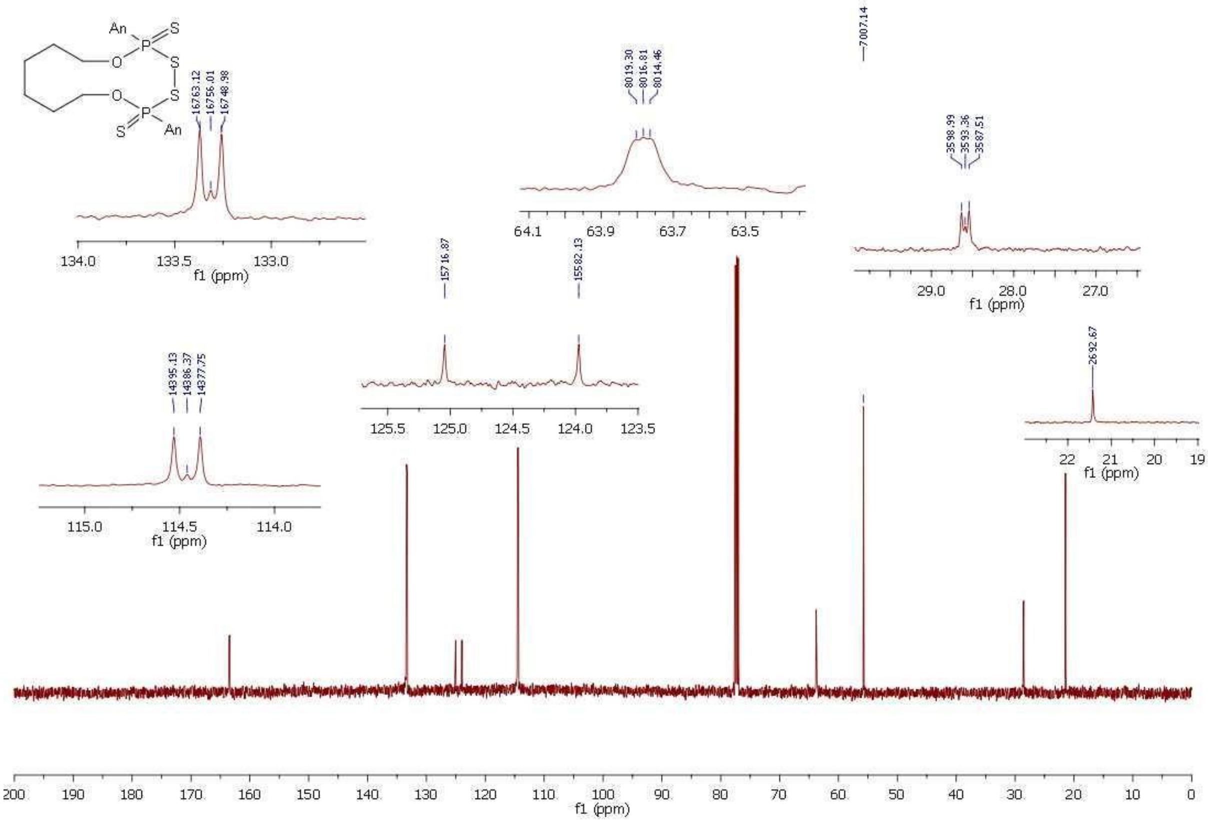

Figure S5. ^{13}C NMR spectrum of **2d** in $CDCl_3$

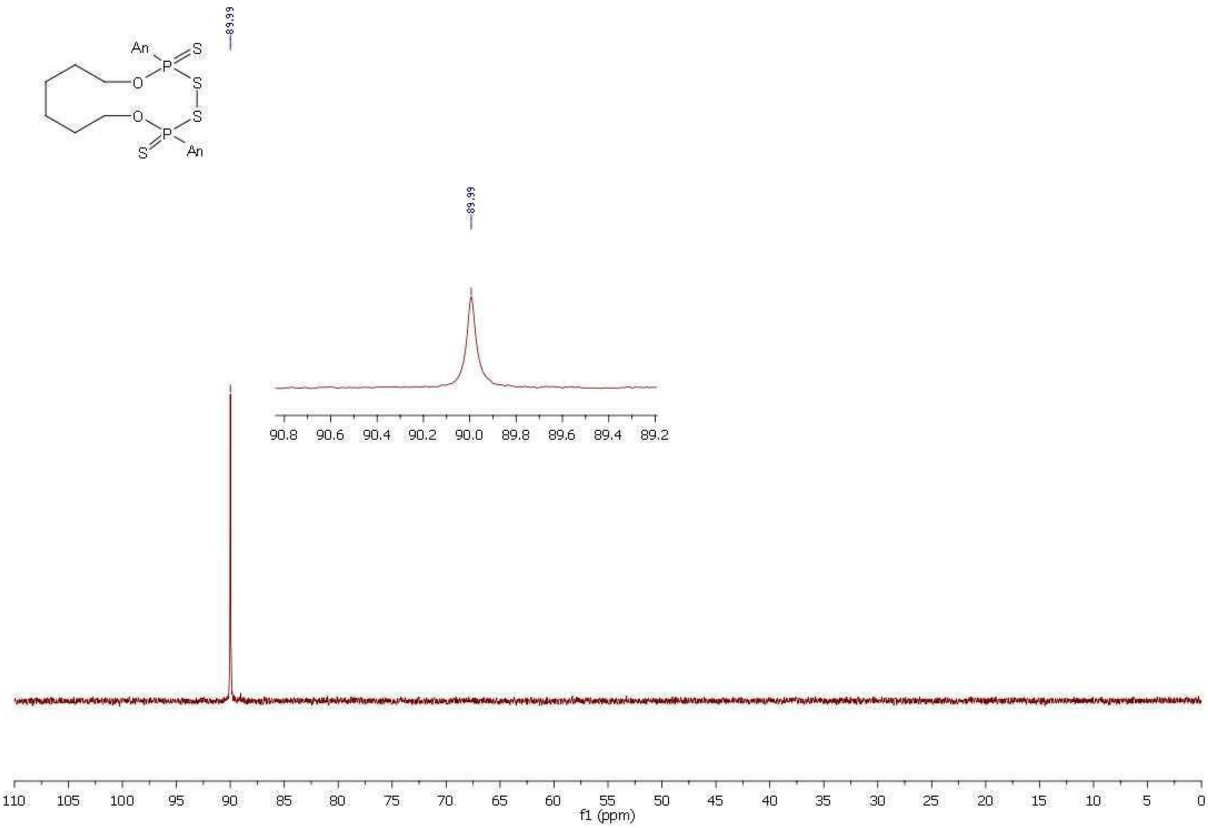

Figure S6. ^{31}P NMR spectrum of **2d** in $CDCl_3$

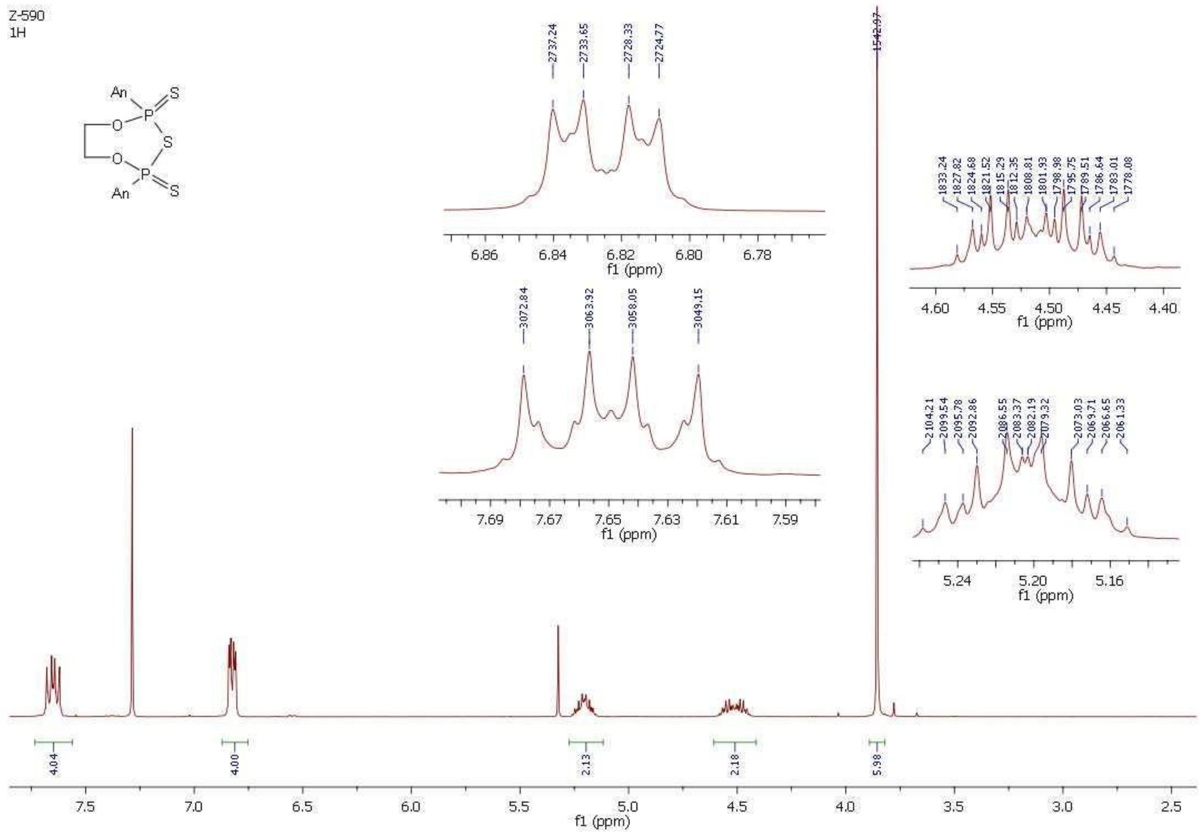

Figure S7. ^{1}H NMR spectrum of *cis*-**3a** in $CDCl_3$

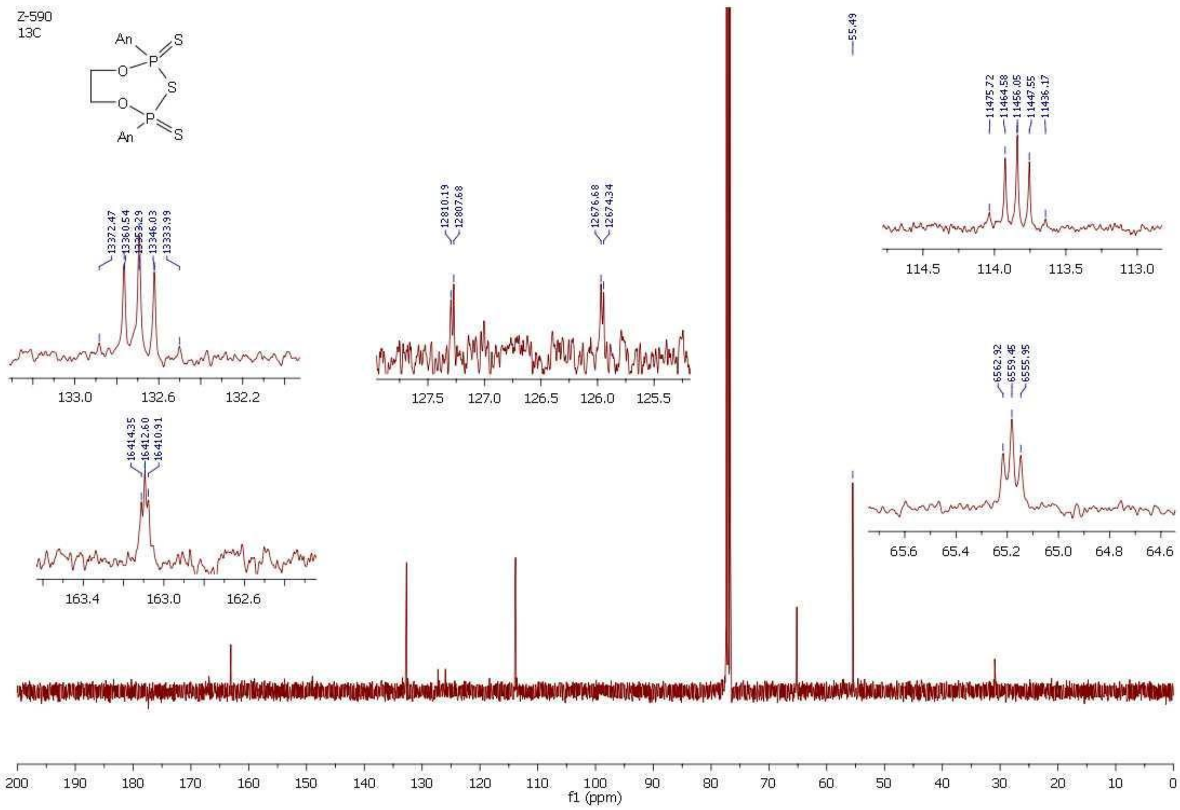

Figure S8. ^{13}C NMR spectrum of *cis*-**3a** in $CDCl_3$

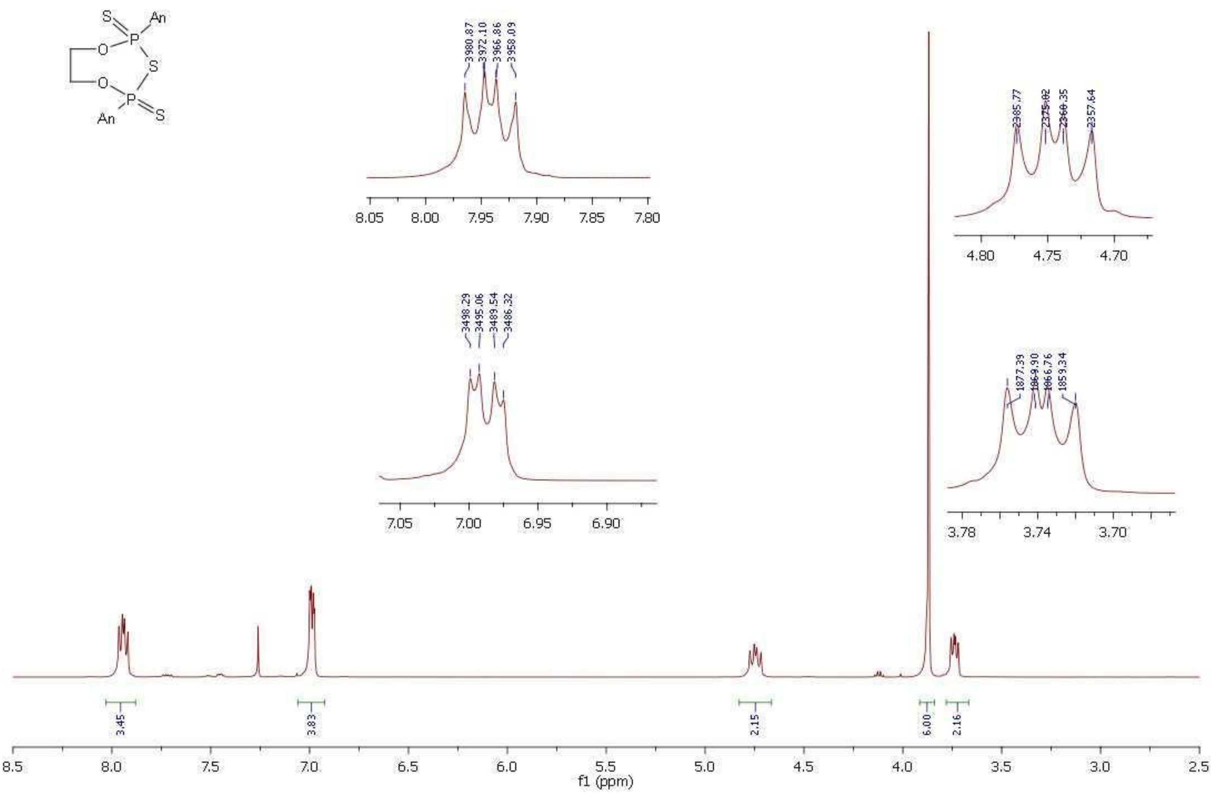

Figure S9. ^1H NMR spectrum of *trans*-**3a** in $CDCl_3$

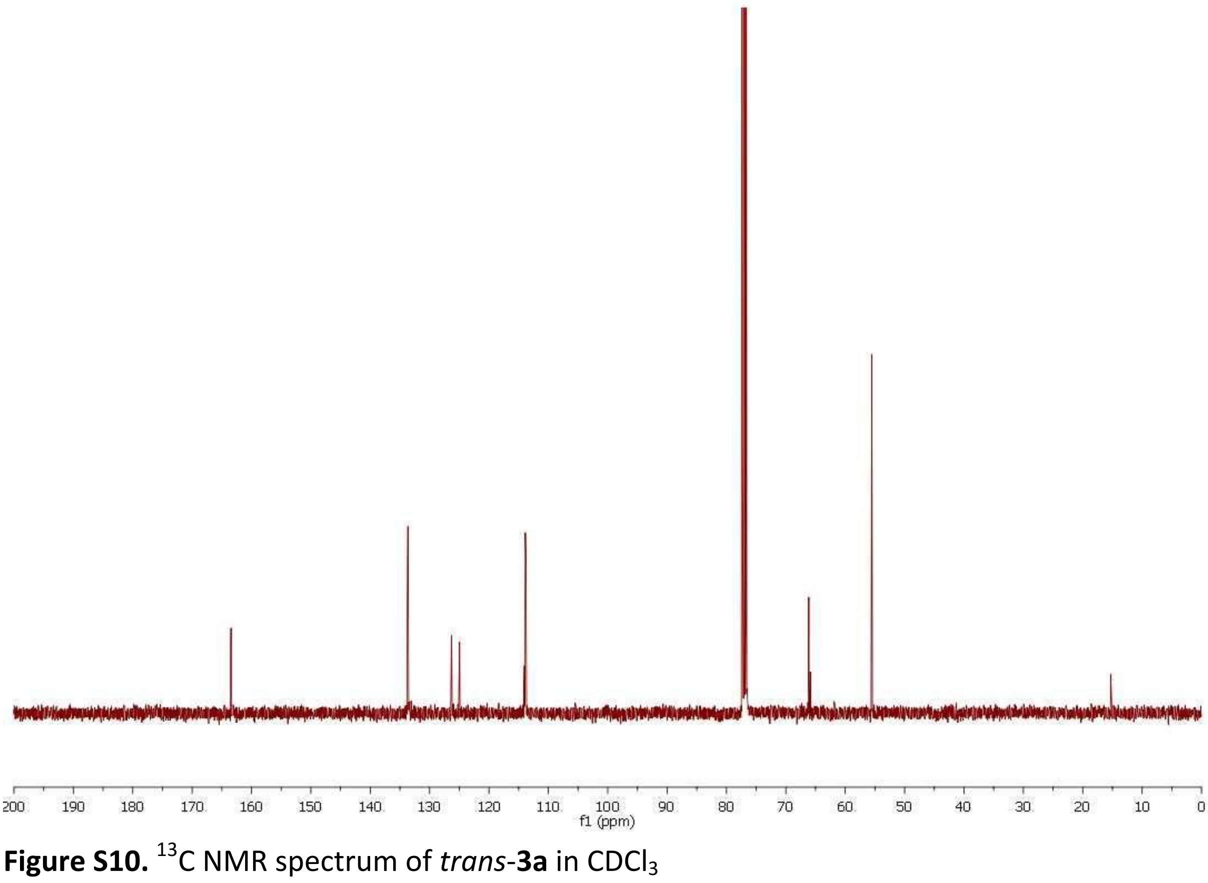

Figure S10. ^{13}C NMR spectrum of *trans*-**3a** in $CDCl_3$

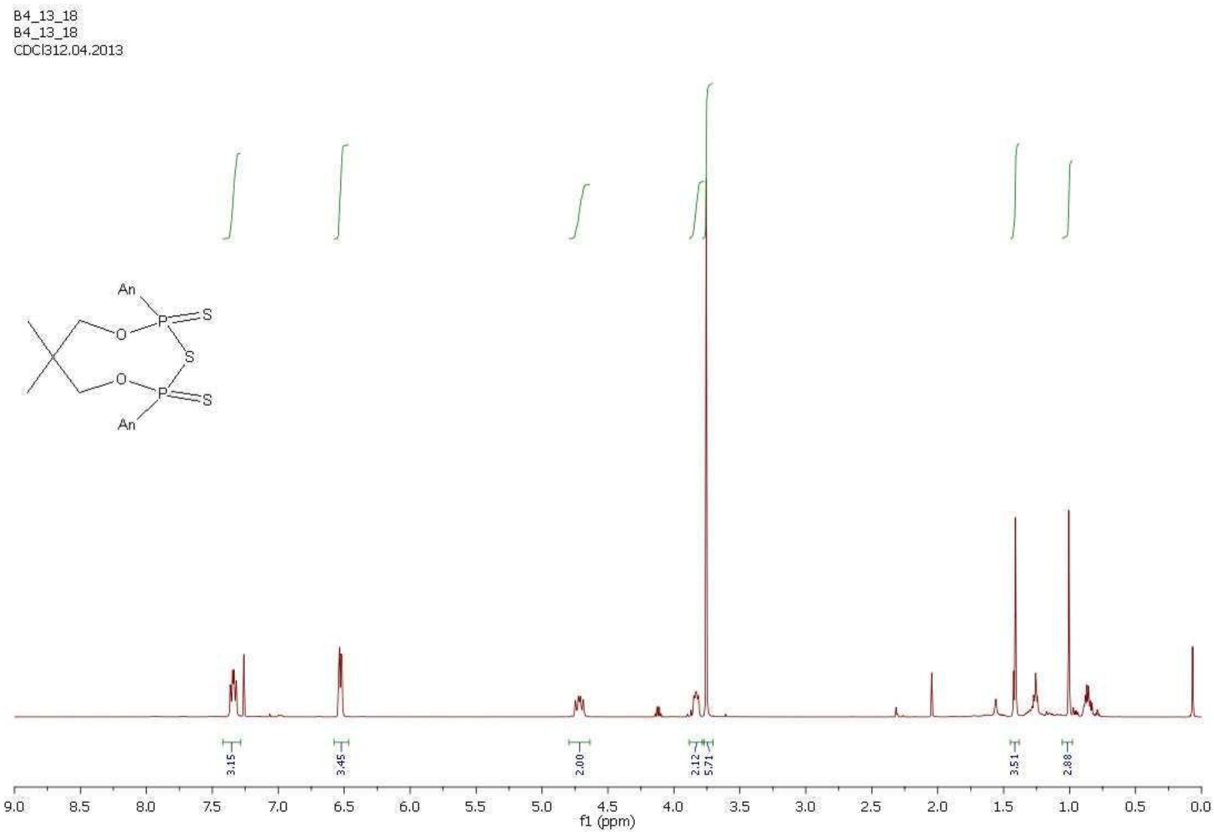

Figure S11. ^{1}H NMR spectrum of *cis*-**3b** in $CDCl_3$

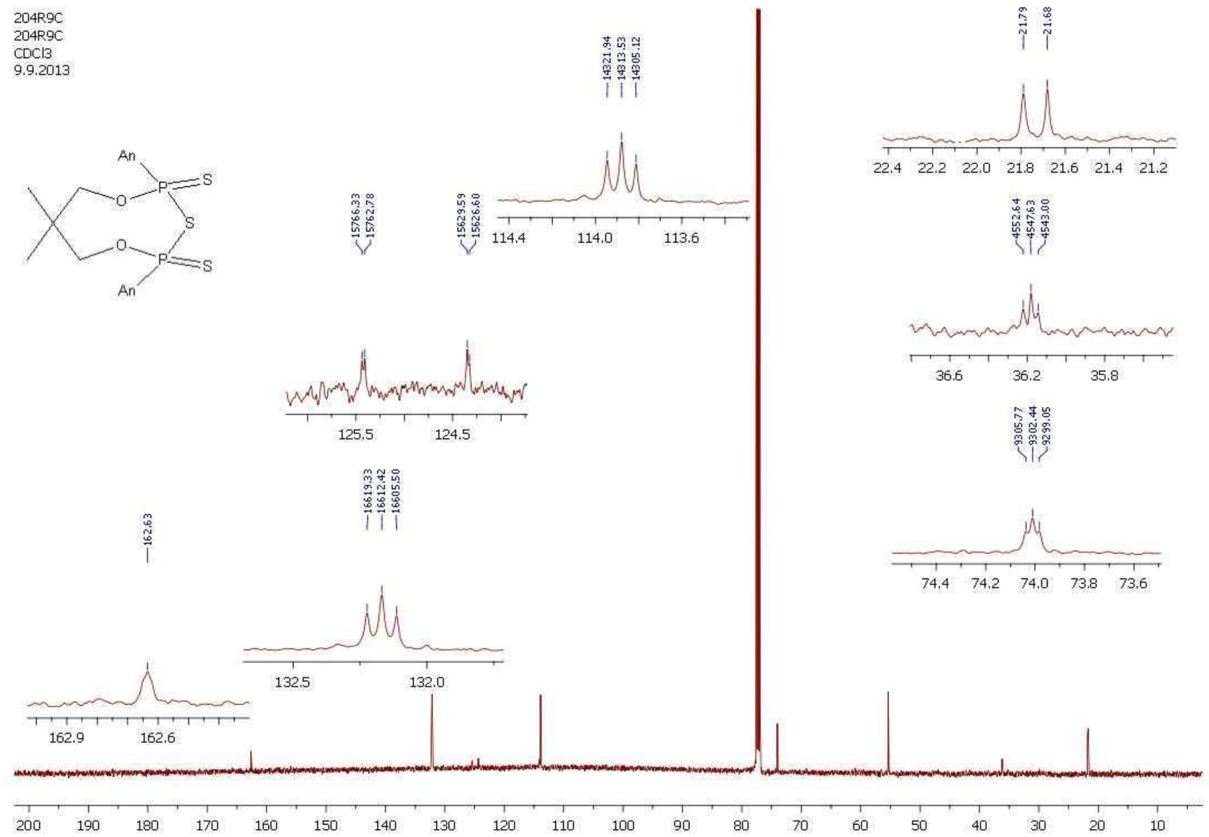

Figure S12. ^{13}C NMR spectrum of *cis*-**3b** in $CDCl_3$

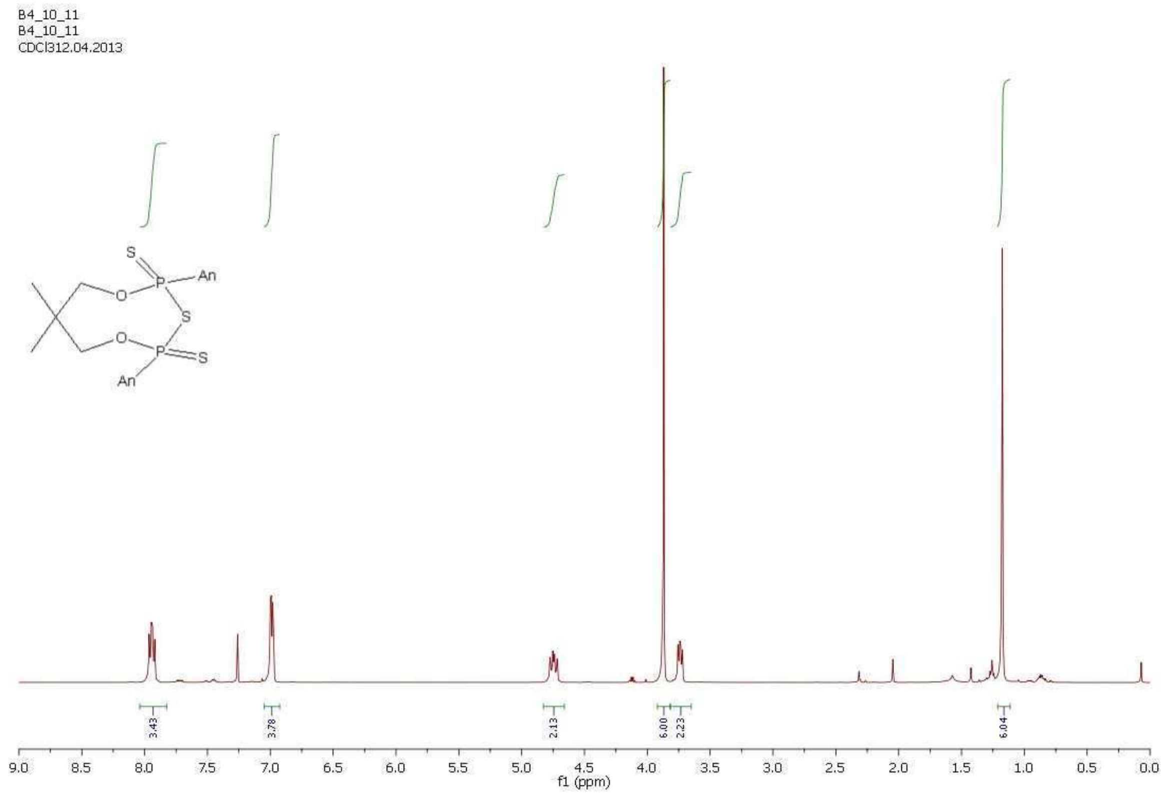

Figure S13. ^{1}H NMR spectrum of *trans*-**3b** in $CDCl_3$

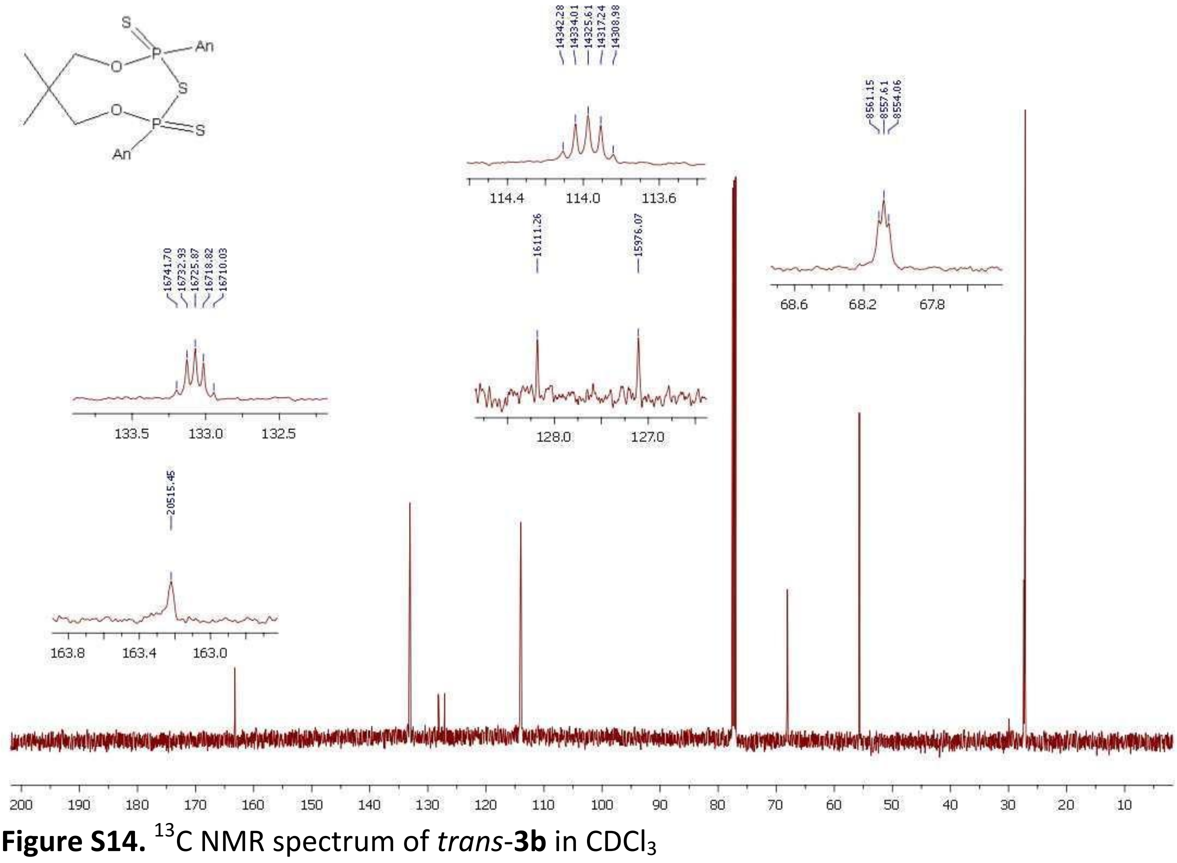

Figure S14. ^{13}C NMR spectrum of *trans*-**3b** in $CDCl_3$

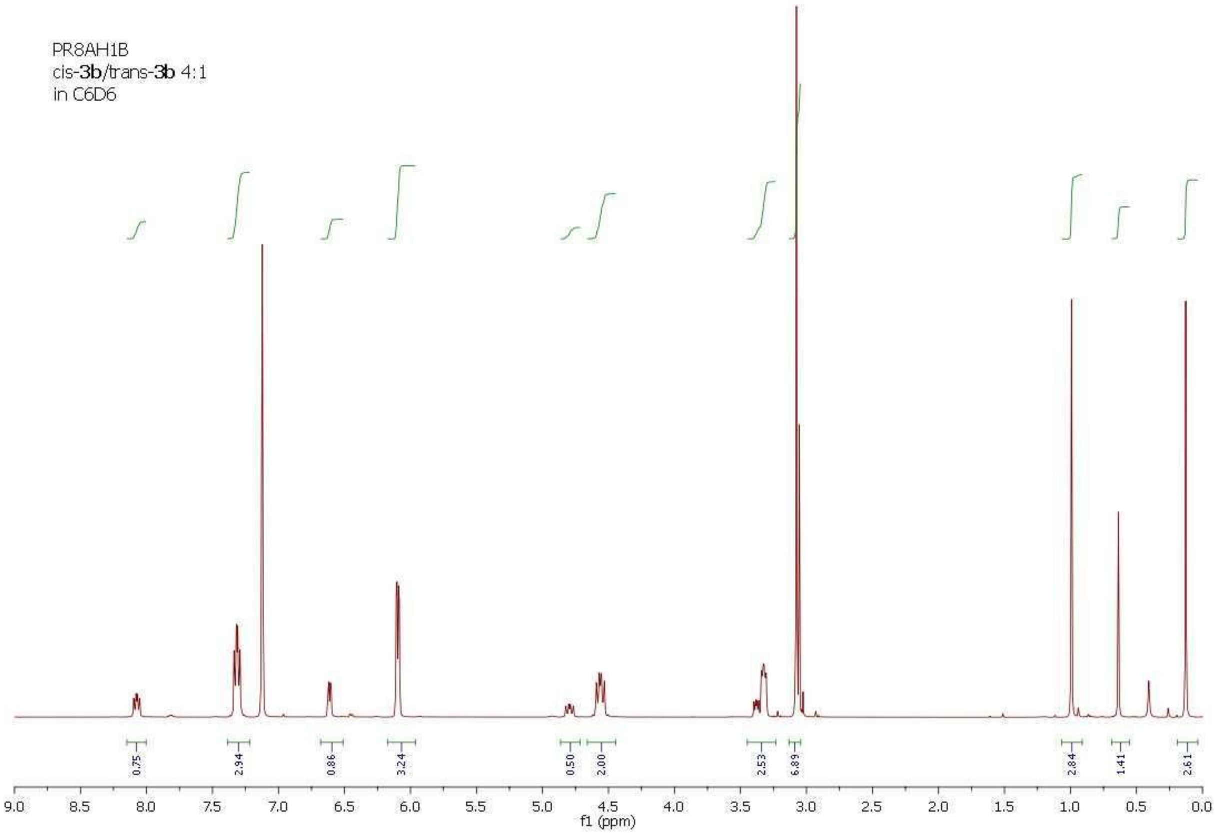

Figure S15. ^{1}H NMR spectrum of a crude mixture of *cis*-**3b** and *trans*-**3b** (4:1) in C_6D_6

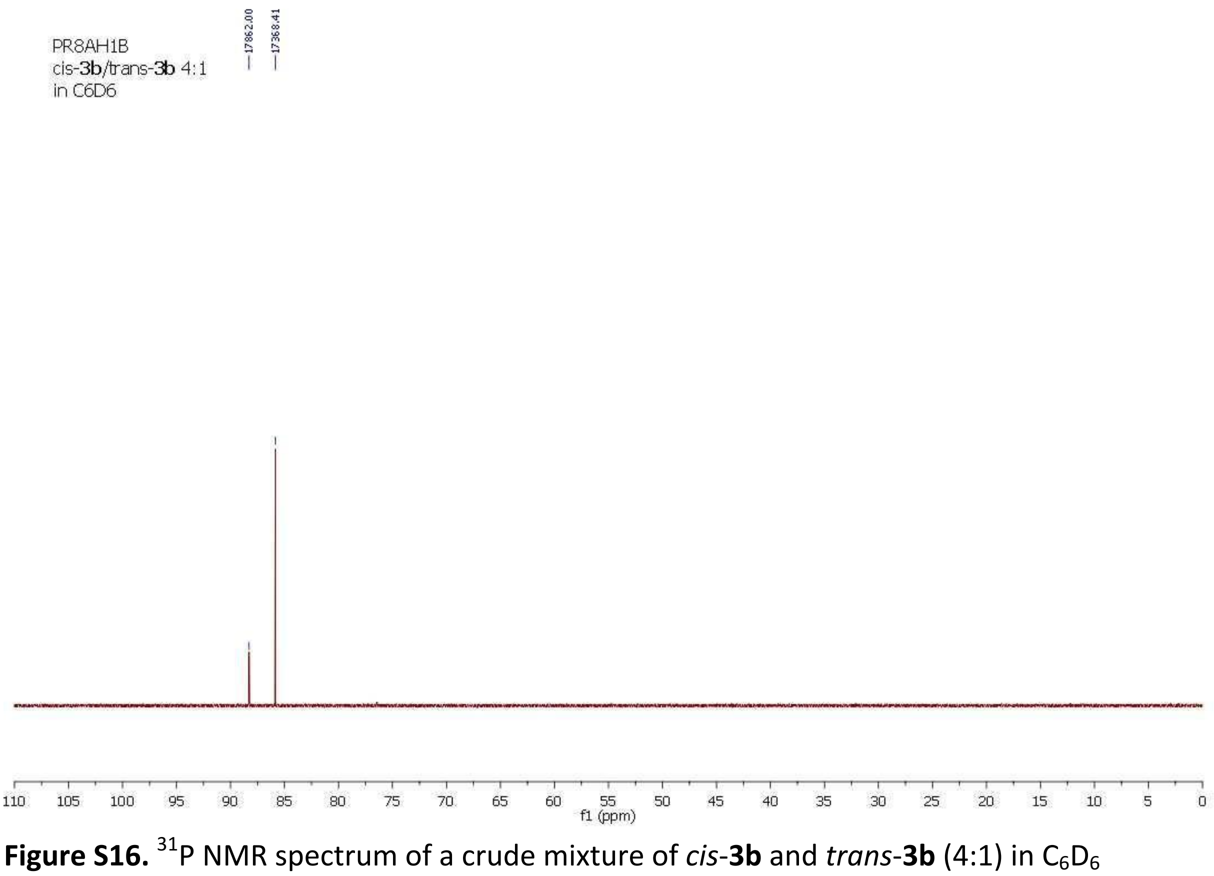

Figure S16. ^{31}P NMR spectrum of a crude mixture of *cis*-**3b** and *trans*-**3b** (4:1) in C_6D_6

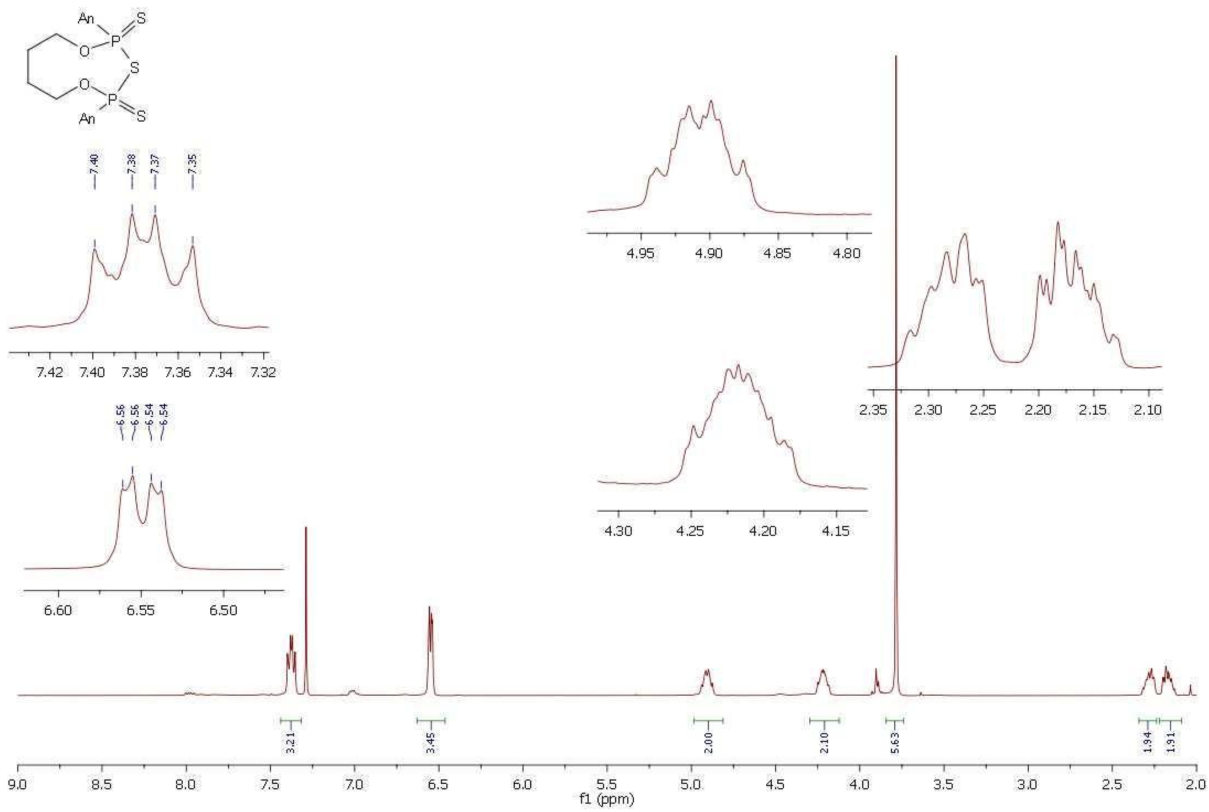

Figure S17. ^{1}H NMR spectrum of *cis*-**3c** in $CDCl_3$

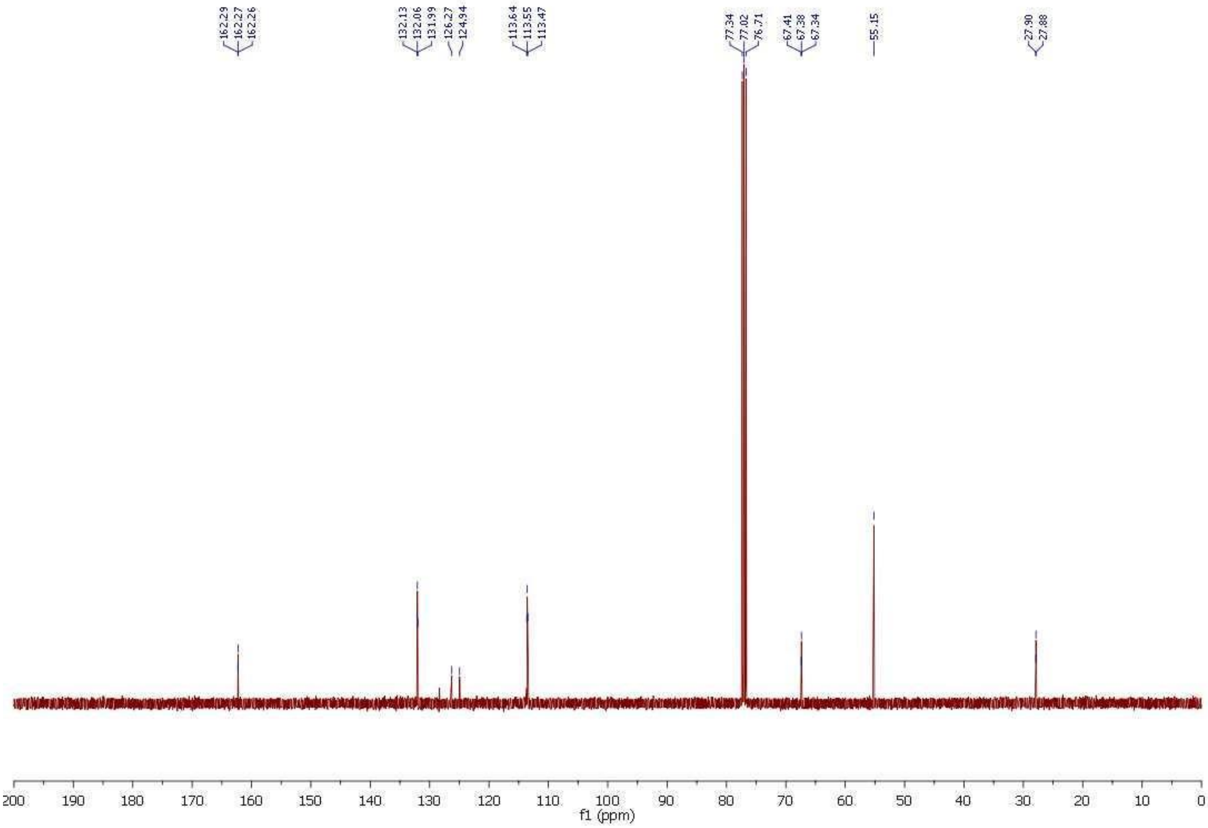

Figure S18. ^{13}C NMR spectrum of *cis*-**3c** in $CDCl_3$

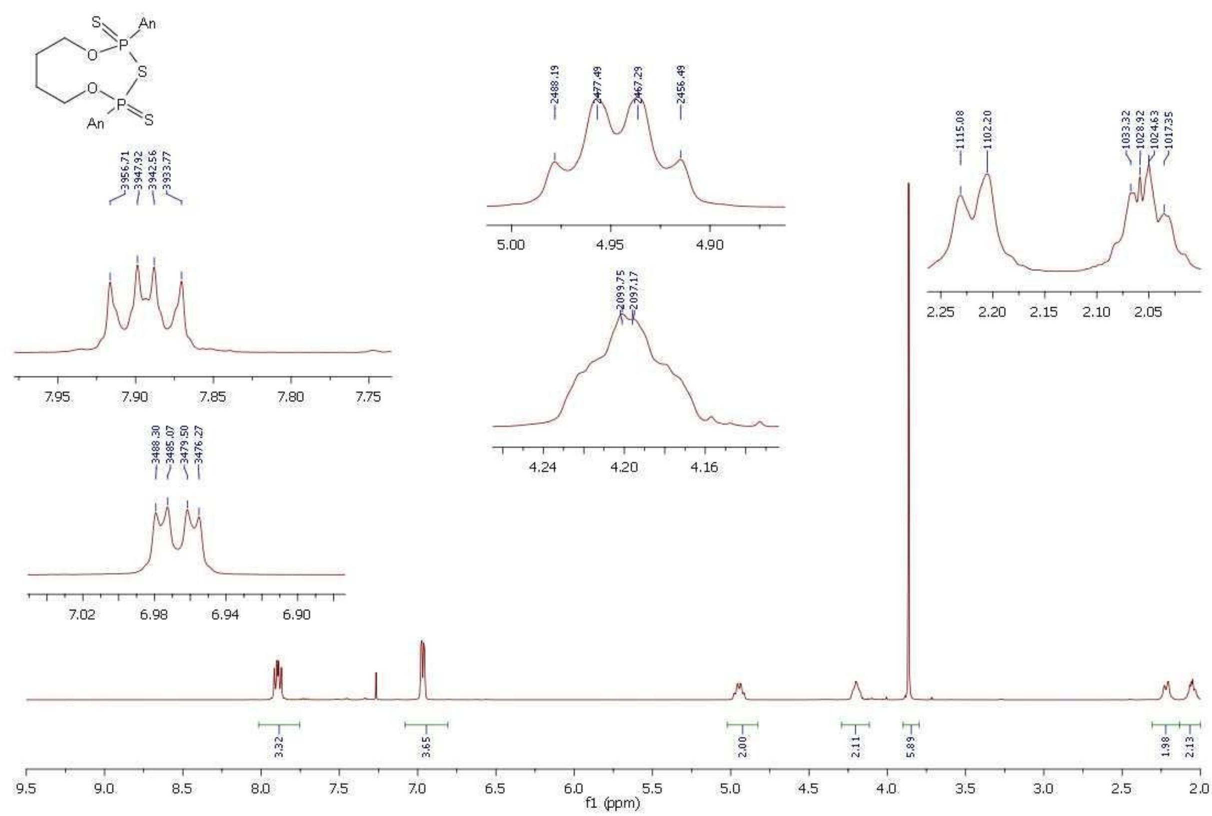

Figure S19. ^{1}H NMR spectrum of *trans*-**3c** in $CDCl_3$

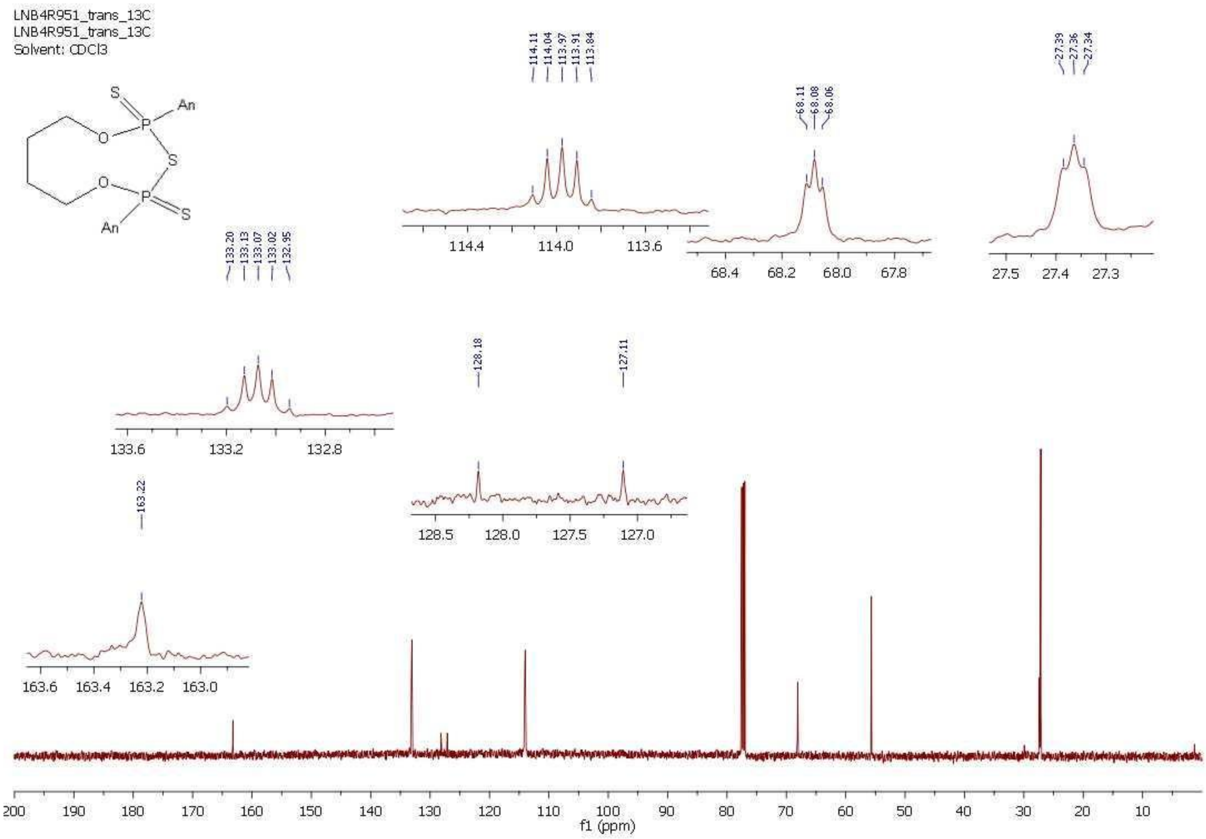

Figure S20. ^{13}C NMR spectrum of *trans*-**3c** in $CDCl_3$

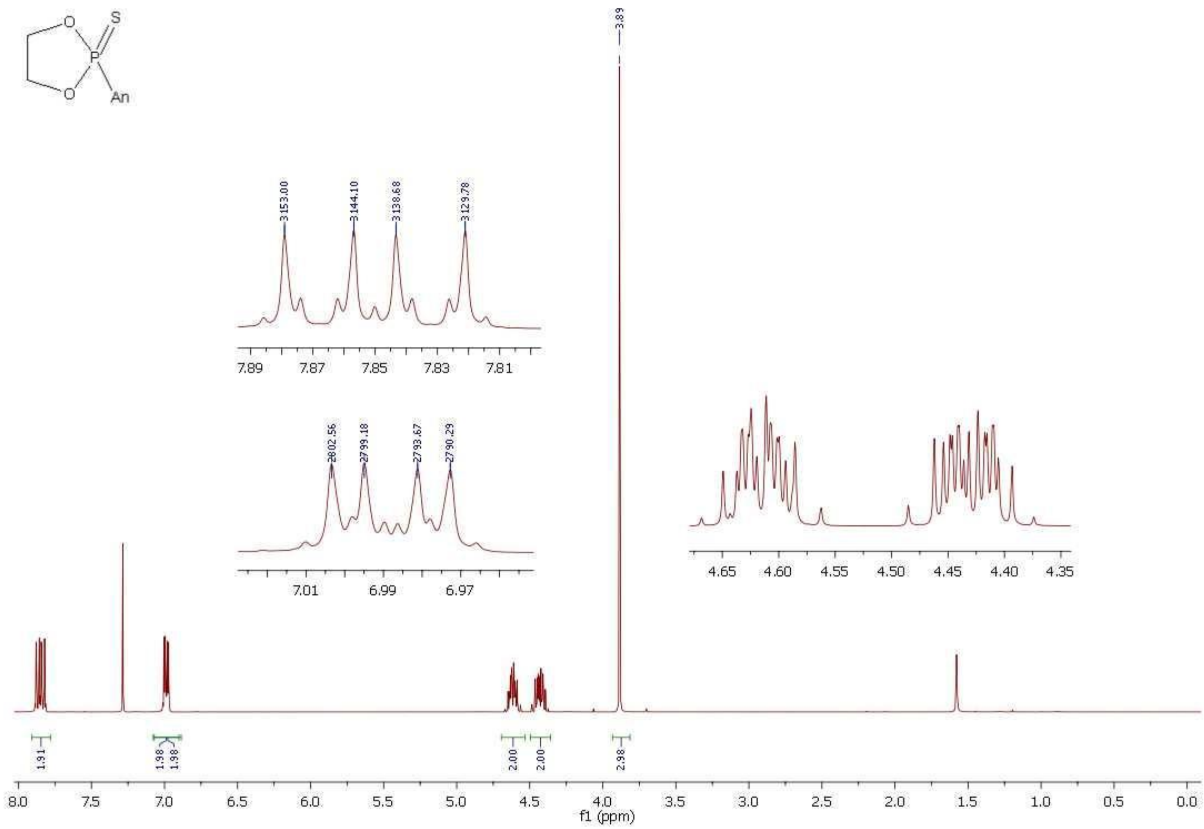

Figure S21. ^{1}H NMR spectrum of **4a** in $CDCl_3$

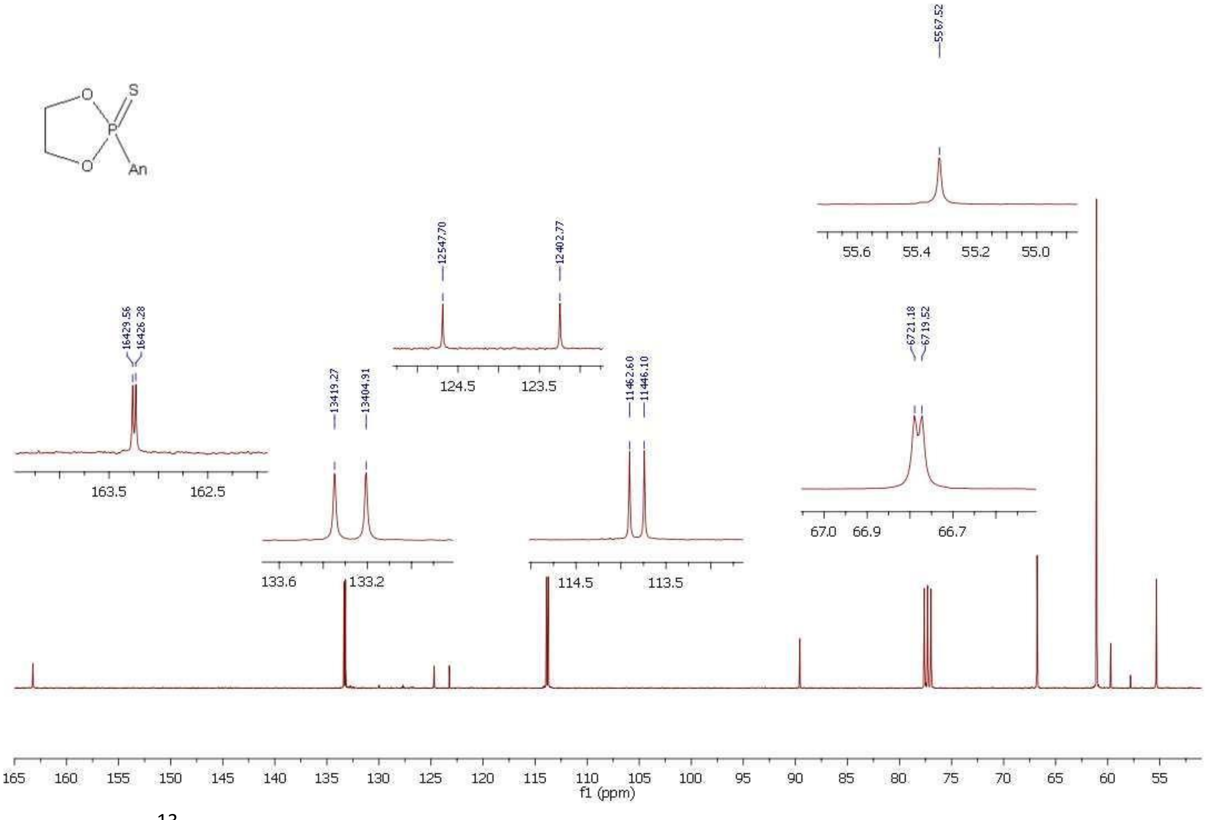

Figure S22. ^{13}C NMR spectrum of **4a** in $CDCl_3$

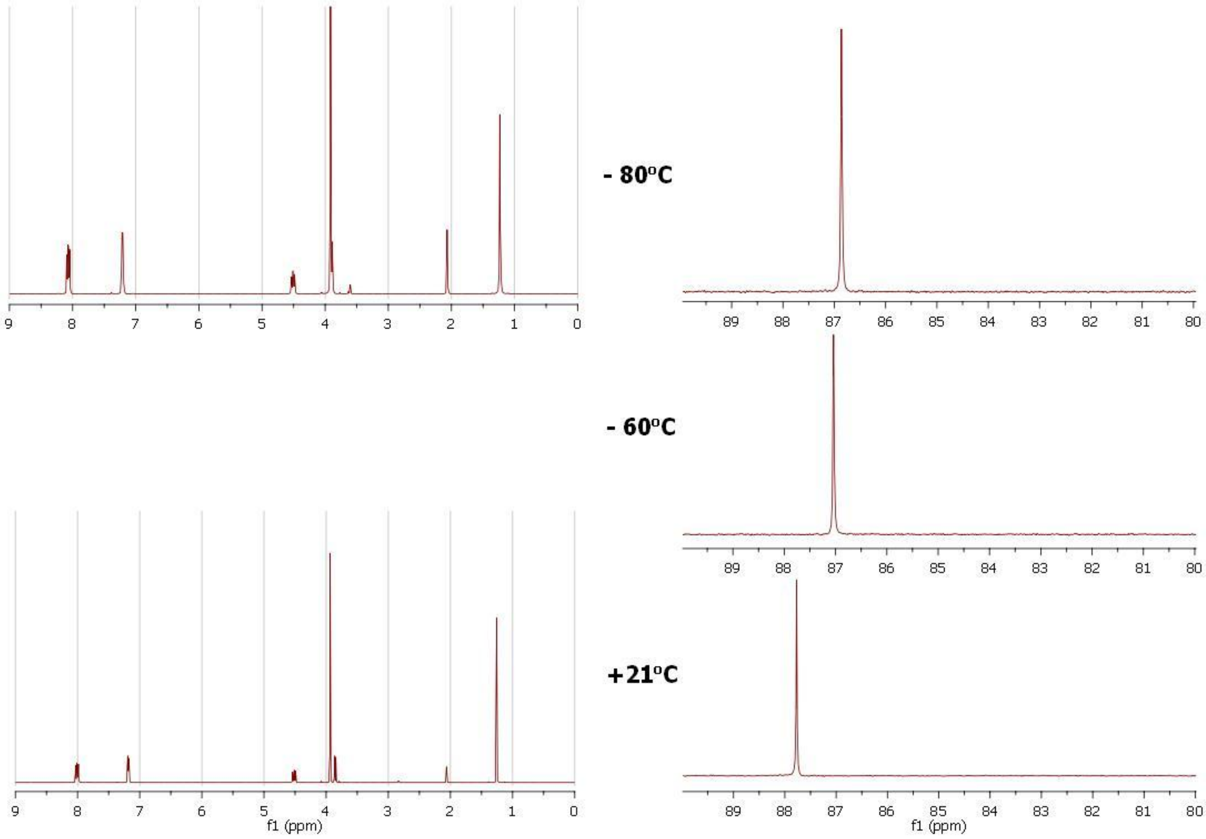

Figure S23. Comparing the ^{1}H NMR (a-b) and ^{31}P NMR (c-e) spectra of disulfane **2b** solution in acetone-d_6 recorded at cryogenic temperatures and at room temperature.

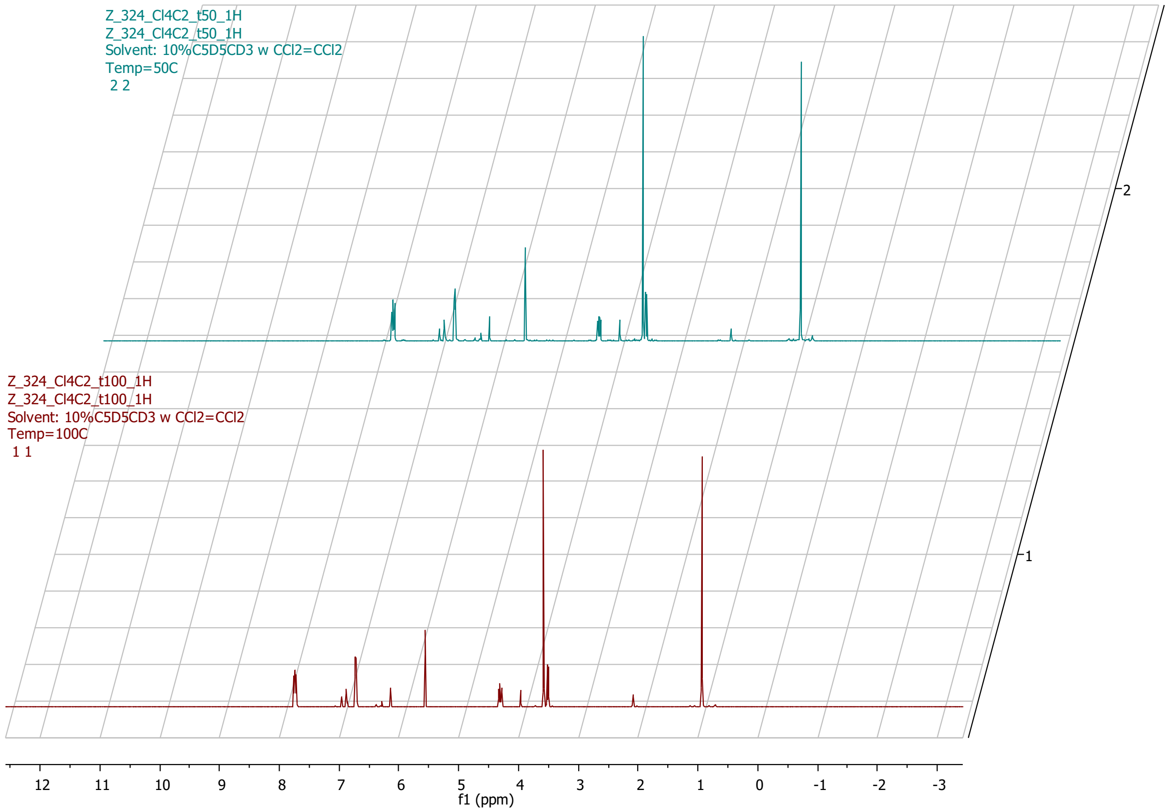

Figure S24. [1]H NMR spectra of **2b** in C_2Cl_4 recorded at a) 50°C and b) 100°C

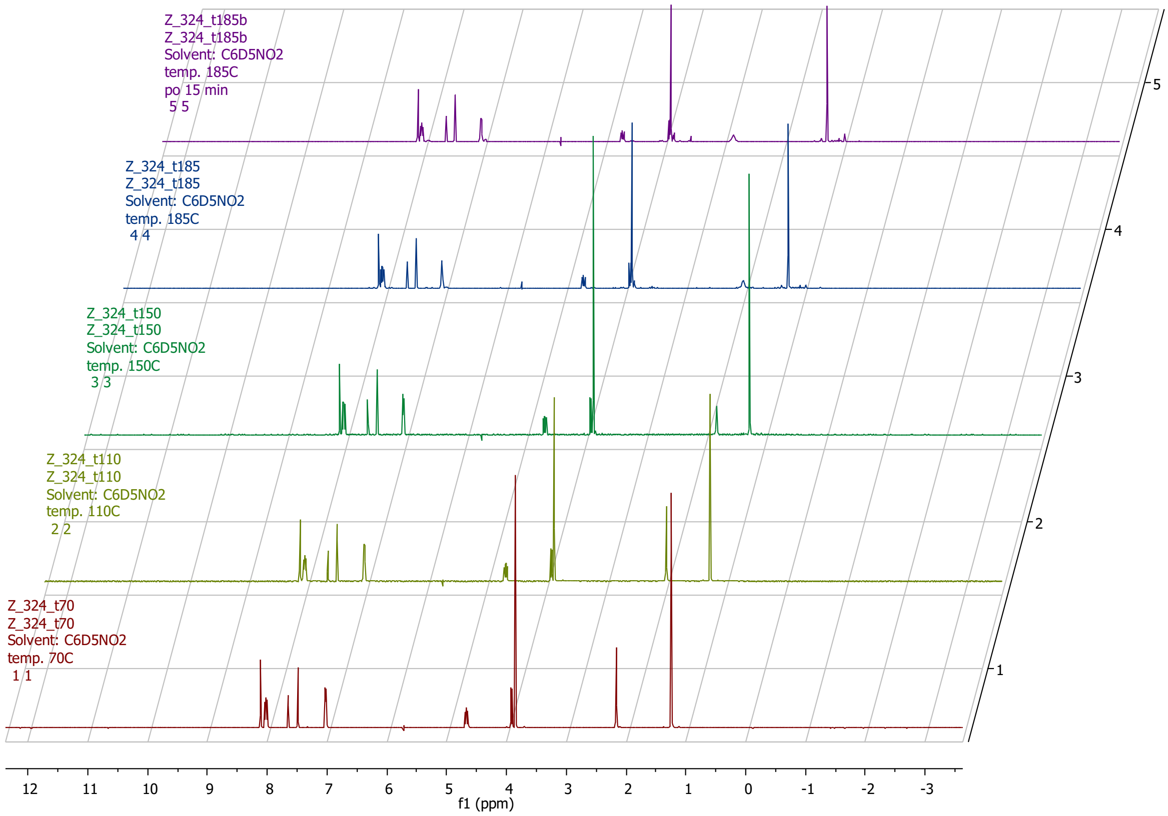

Figure S25. [1]H NMR spectra of **2b** in $C_5D_6NO_2$ recorded at (a) 70°C, (b) 110°C, (c) 150°C, (d) 185°C and (e) 185°C for 15 min

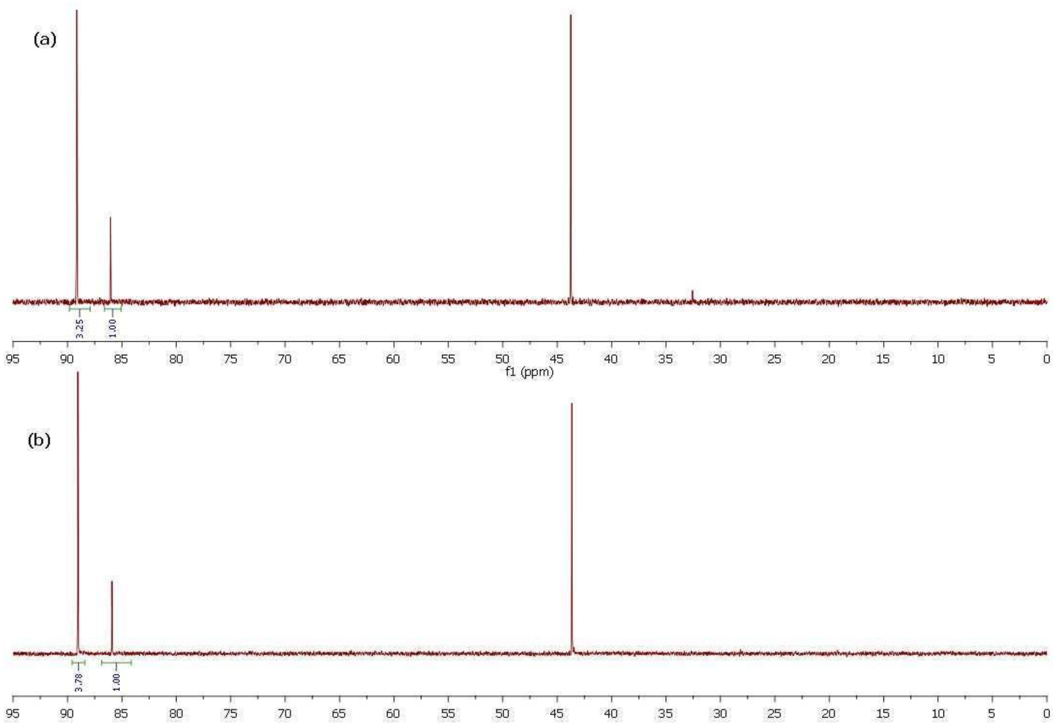

Figure S26. 202 MHz ^{31}P NMR spectra of the crude reaction mixture of disulfane **2a** and Ph_3P: (a) alone (b) after administration of 1 eq of 2,4-dinitrobenzoic acid in CH_2Cl_2 plus 10% C_6D_6

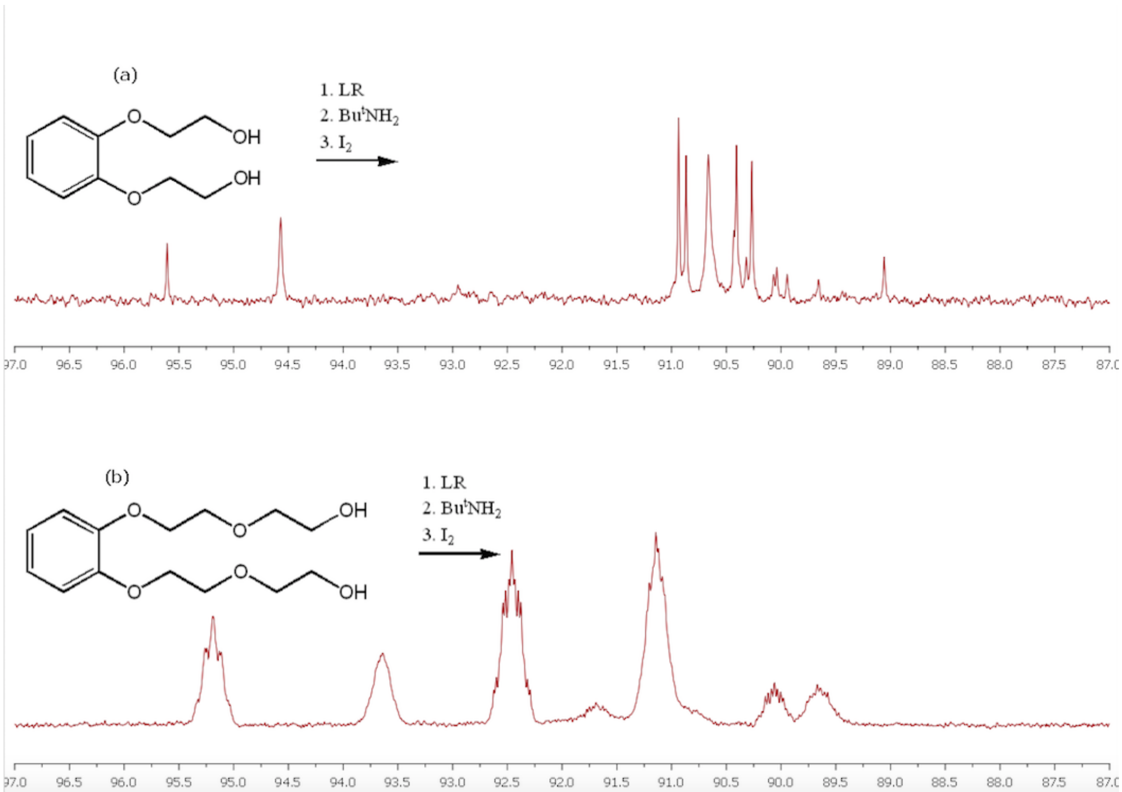

Figure S27. ^{31}P NMR spectra of reaction products obtained using the general procedure (see experimental section), which was intended to give rise to: (a) 14- (^1H decoupled spectrum) and (b) 20-membered disulfanes (non-decoupled spectrum)

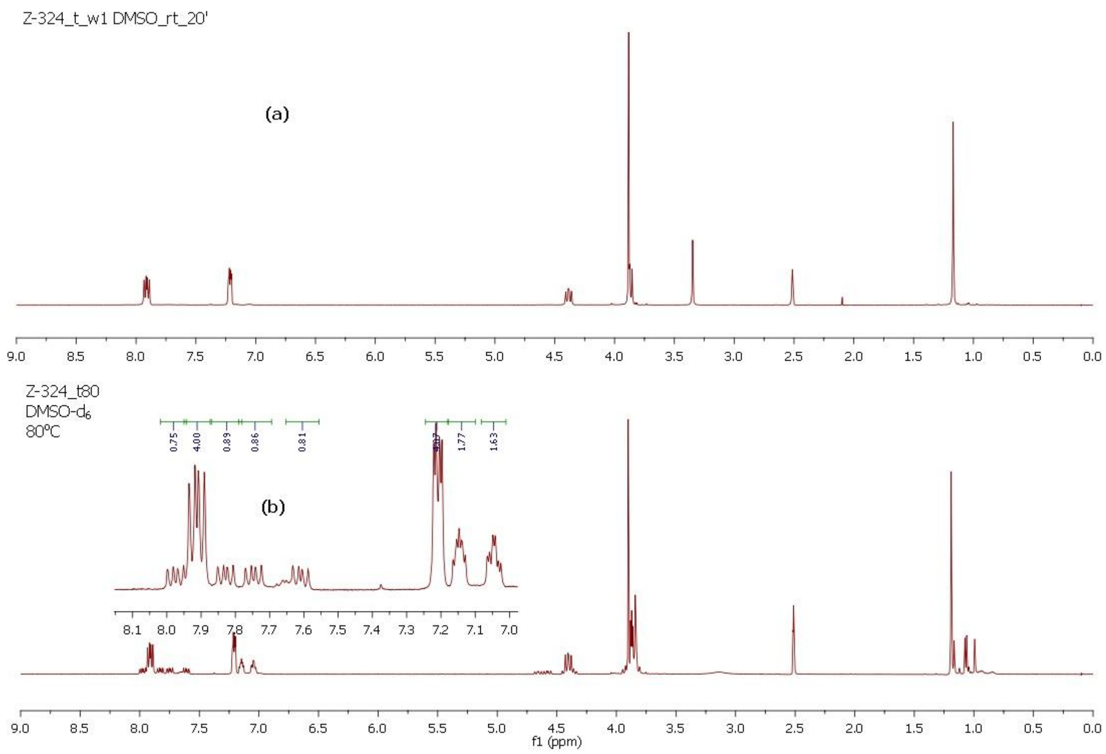

Figure S28. 202 MHz ^{31}P NMR spectra of the solution of disulfane **2b** in DMSO-d_6 showing the presence of **2b** S-oxides as its initial oxidation products.

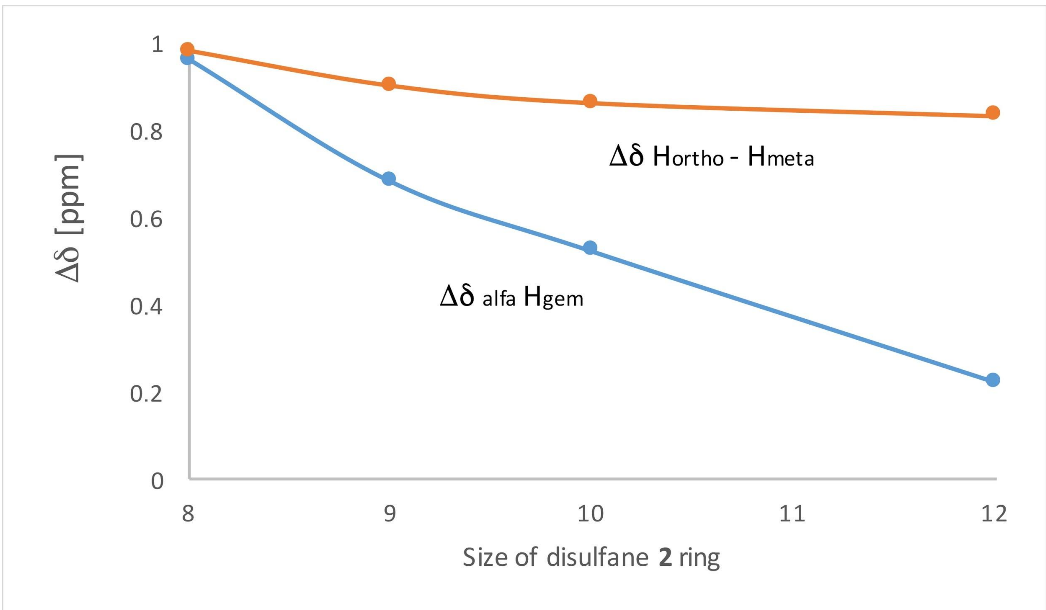

Figure S29. Correlations of cyclic disulfanes **2** (except for **2b'**) ring size and the difference in chemical shifts for geminal protons $\Delta\delta_{Hax\text{-}Heq}$ (blue line) and for aromatic $\Delta\delta_{Hortho\text{-}Hmeta}$ protons (red line) taken from NMR spectra recorded in $CDCl_3$ at room temperature.

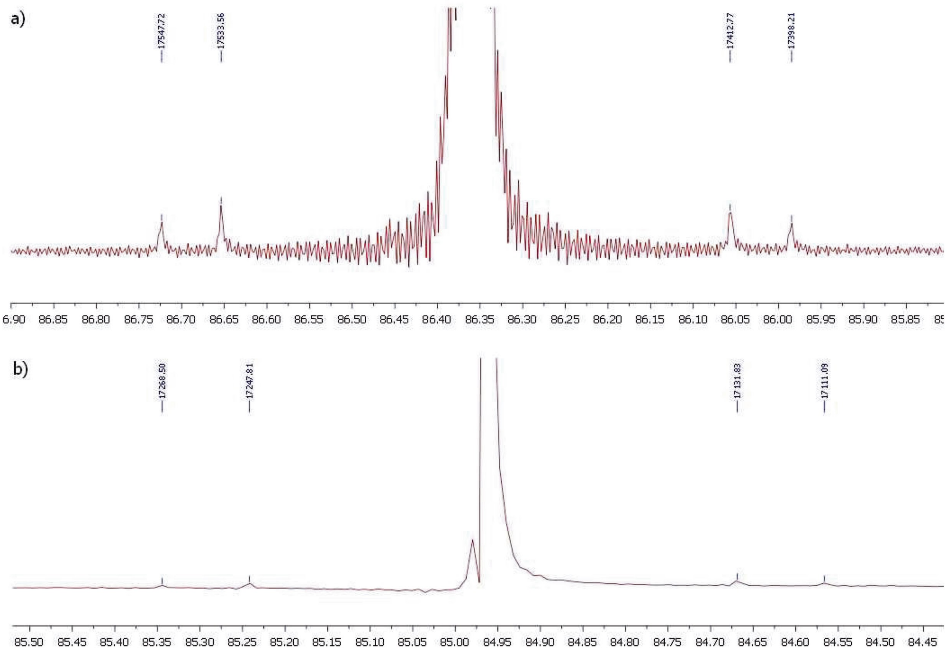

Figure S30. 202 MHz ^{31}P NMR spectra of sulfane **3c** isomers containing ^{13}C satellites showing a difference in P-P couplings: a) *cis*-**3c** (dd, $^{1}J_{PC}$ = 135 Hz, $^{2}J_{PP}$ = -19.3 Hz) and b) *trans*-**3c** (dd, $^{1}J_{PC}$ = 135 Hz, $^{2}J_{PP}$ = -12.8 Hz).

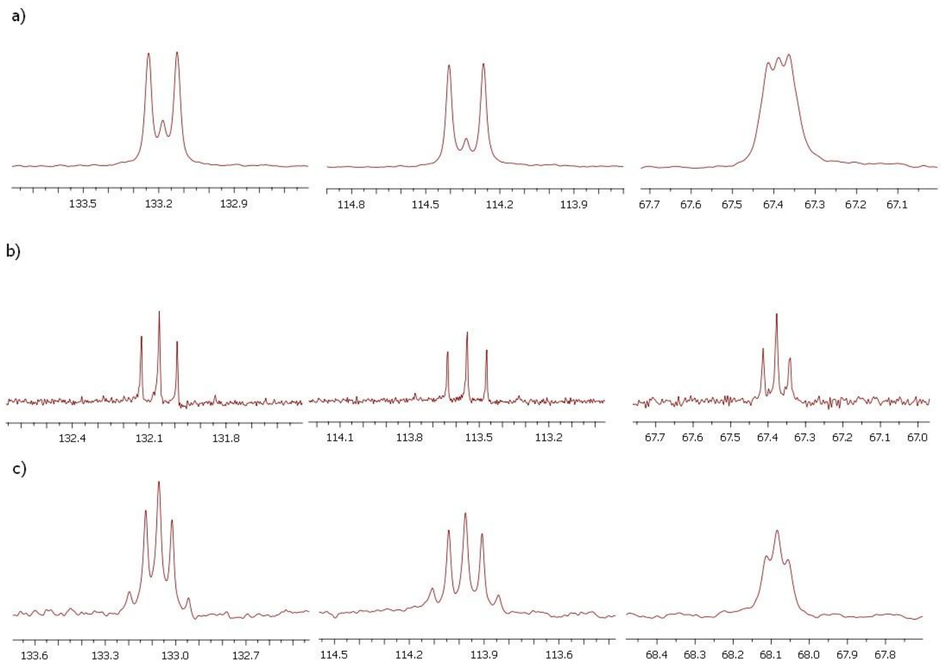

Figure S31. AA’X (OCH_2), C2’ and C3’ false multiplets observed in ^{13}C NMR spectra of (a) disulfane **2c** ($^{3}J_{PP}$ = 4 Hz), (b) sulfane *cis*-**3c** ($^{2}J_{PP}$ = -21 Hz), and sulfane *trans*-**3c** ($^{2}J_{PP}$ = -14 Hz) caused by second-order effects of phosphorus atoms magnetic non-equivalence.

Table S1 Calculated and experimental ^{31}P NMR parameters for cyclic **2** and **3**

	P1/P2 absolute magnetic shielding σ_x calcd	^{31}P Chem shift Calcd* (mean value) $\delta_x = \sigma_{std} - \sigma_x$	^{31}P Chem shift Exp	$^nJ_{PP}$ Calcd	$^nJ_{PP}$ Exp	$^nJ_{exp}/^nJ_{calc}$
2a	243.3/243.5	98.3	88.0	-0.98	4	4.1
2b	234.9/242.4	102.8	88.7	-1.33	4	3.0
2c	237.7/246.5	99.4	89.2	-1.20	4	3.0
2d	236.6/237.2	104.6	90.0	-1.56	4	2.6
cis-**3a**	240.1/246.3	98.3	85.9	-6.1	NM	NM
cis-**3b**	242.0/245.4	97.8	86.1	-6.1	NM	NM
cis-**3c**	239.3/246.6	98.5	85.6	-6.3	-20.9	3.3
trans-**3a**	236.4/238.8	103.9	89.0	-5.3	-13.0	2.5
trans-**3b**	242.9/243.8	98.1	87.7	-5.0	-13.0	2.6
trans-**3c**	241.6/243.7	98.8	86.5	-5.0	-12.8	2.8

(*) Relative to a 85% H_3PO_4 standard (σ_{std} = 341.5 ppm)
NM – not measured

IR and Raman spectra

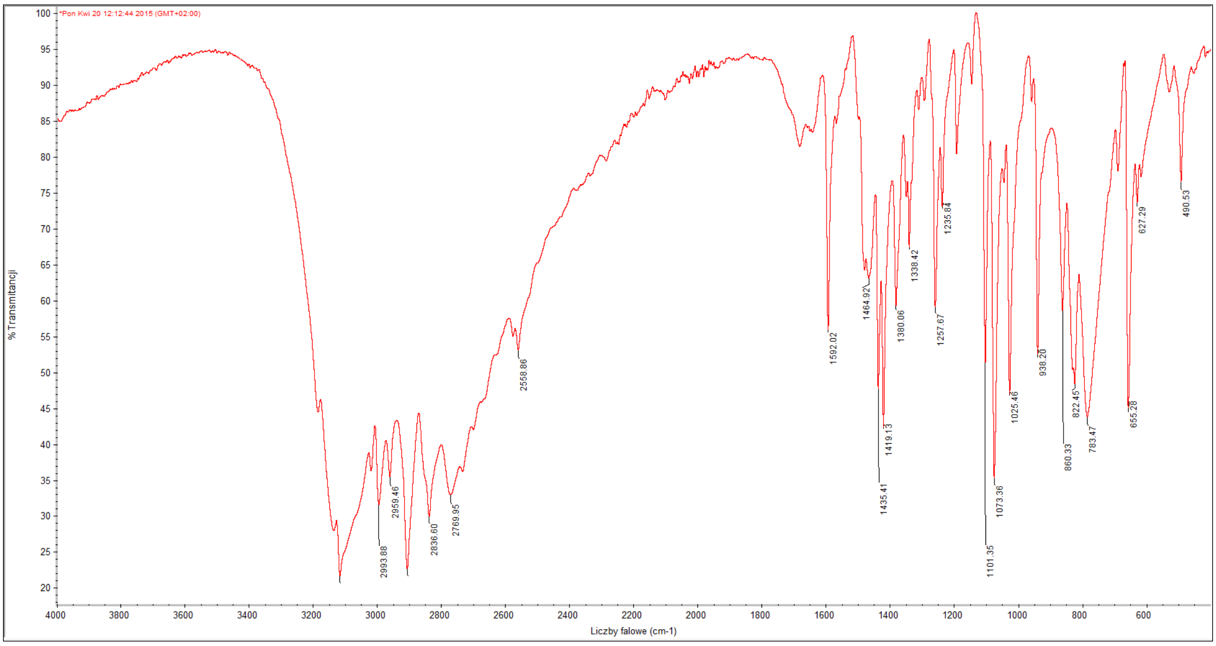

Figure S32. IR spectrum (ATR-IR) of disulfane **2a**

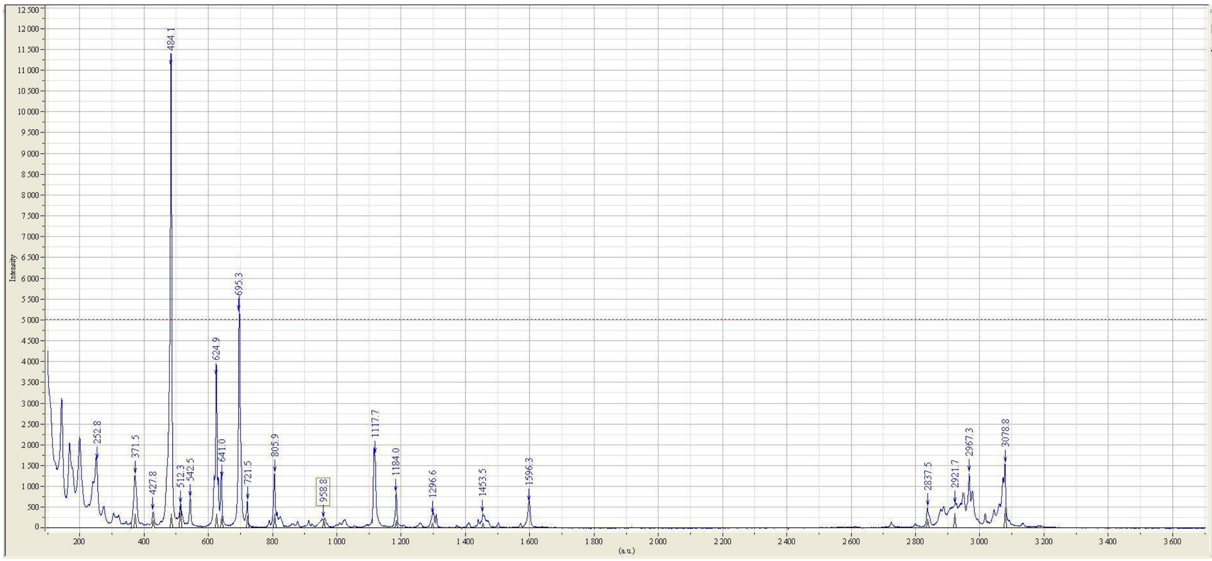

Figure S33. Raman spectrum of disulfane **2a**

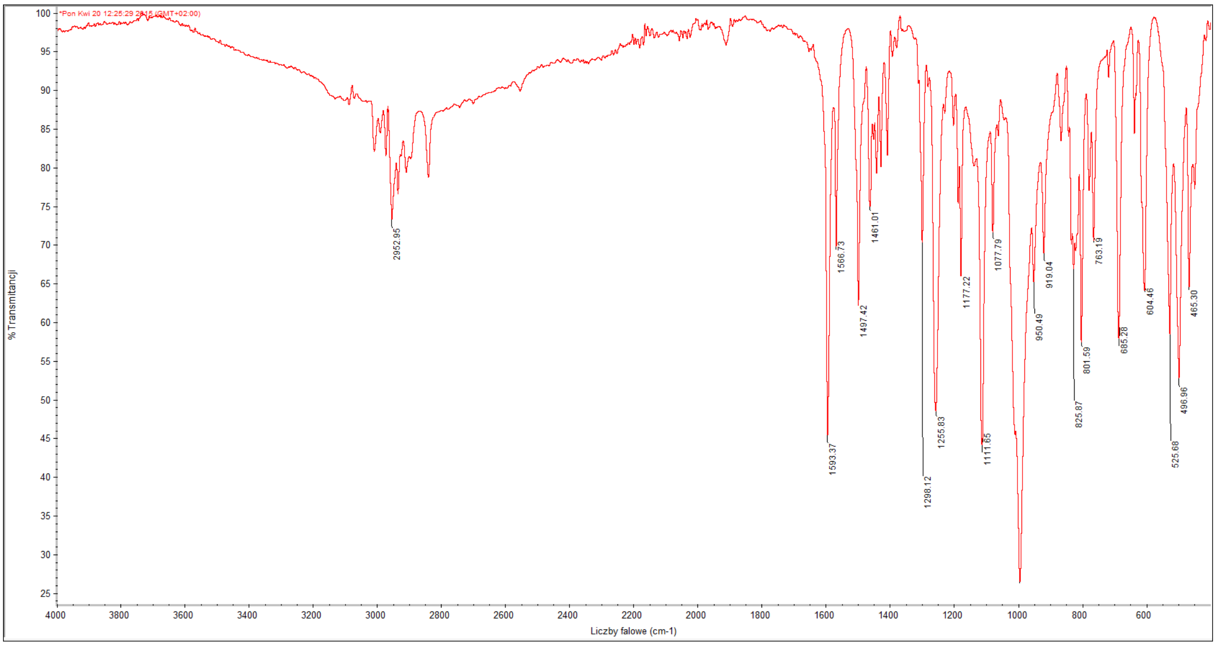

Figure S34. IR spectrum (ATR-IR) of disulfane **2b**

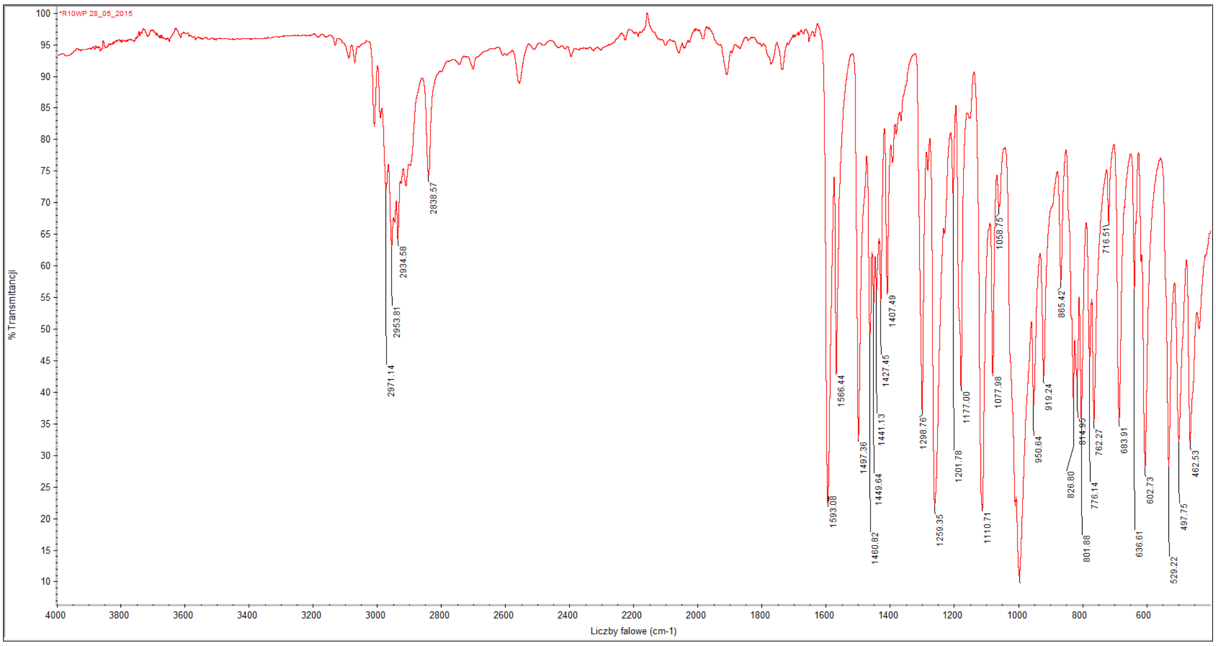

Figure S35. IR spectrum (ATR-IR) of disulfane **2c**

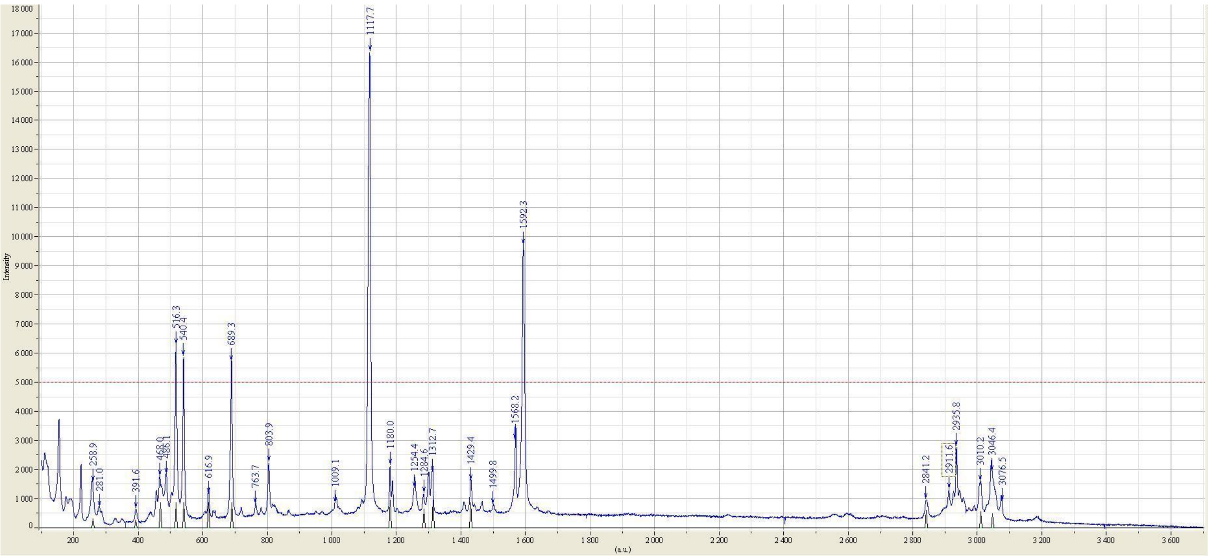

Figure S36. Raman spectrum of disulfane **2c**

X-Ray structural analysis

Crystal structures of cyclic disulfanes **2** and sulfanes **3**

X-ray structures of cyclic disulfanes have been determined for: **2a**, **2b**, **2b'**, **2c** and two polymorphic forms of **2d** – triclinic and monoclinic. Crystallographic data and refinement details are given in **Table S1**. Molecular views of the structures are presented in Figures S37-S-42.

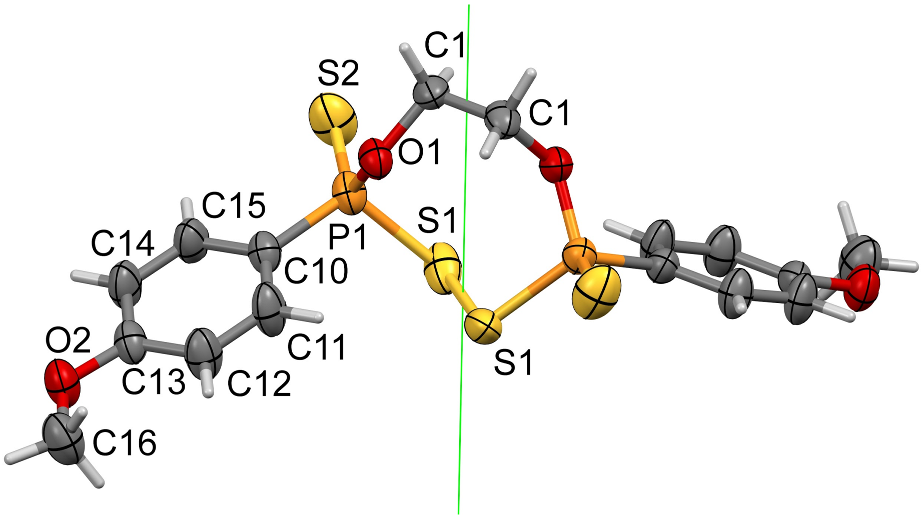

Figure S37. View of structure **2a** showing atom labelling scheme. Symmetry axis drawn as the green line, only two labels for symmetry equivalent atoms shown. Displacement ellipsoids drawn at 50% probability level.

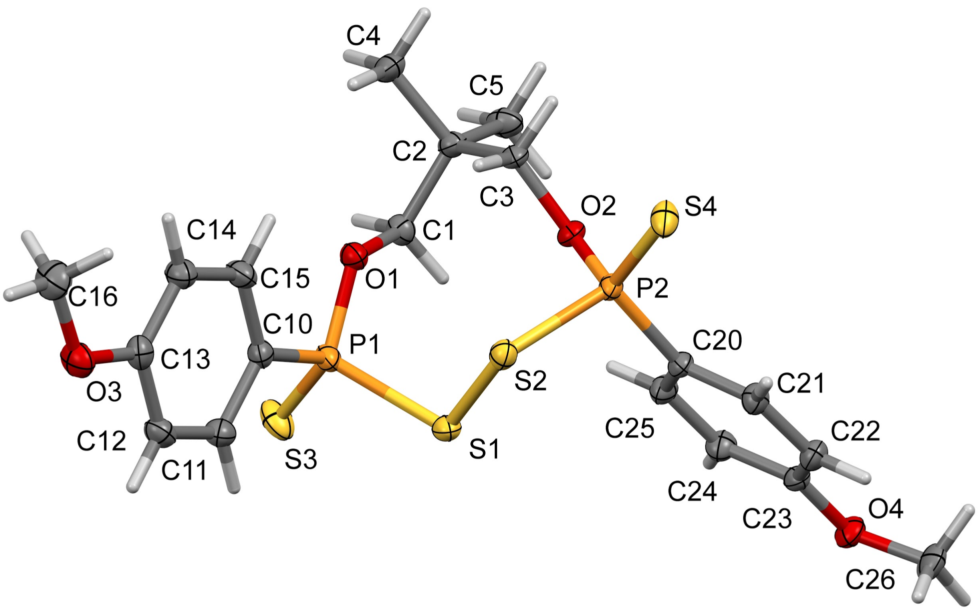

Figure S38. View of asymmetric unit of structure **2b** showing atom labelling scheme. Displacement ellipsoids drawn at 50% probability level

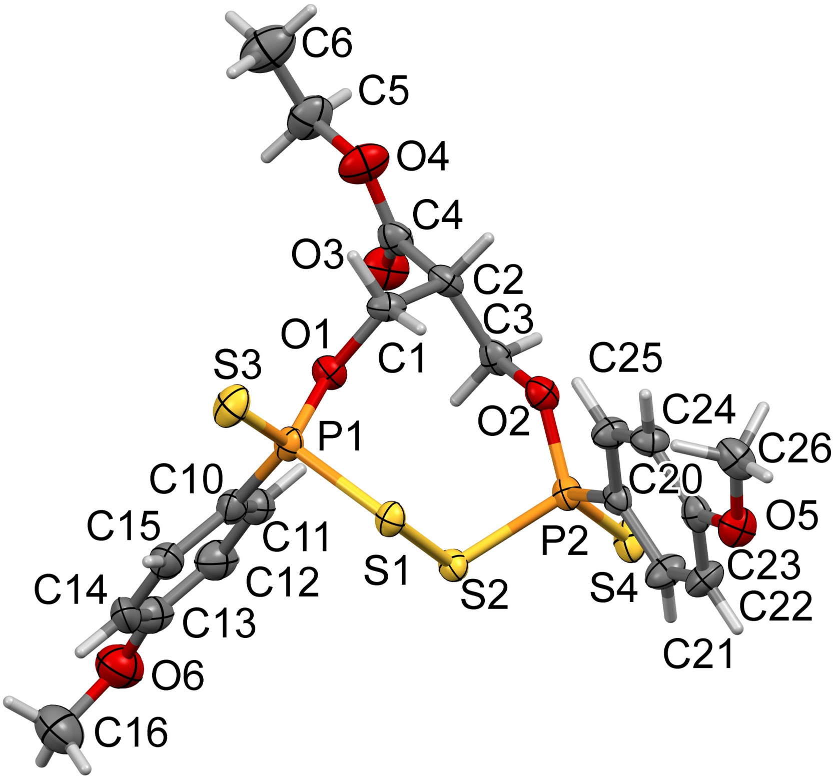

Figure S39. View of asymmetric unit of structure **2b’** showing atom labelling scheme. Displacement ellipsoids drawn at 50% probability level.

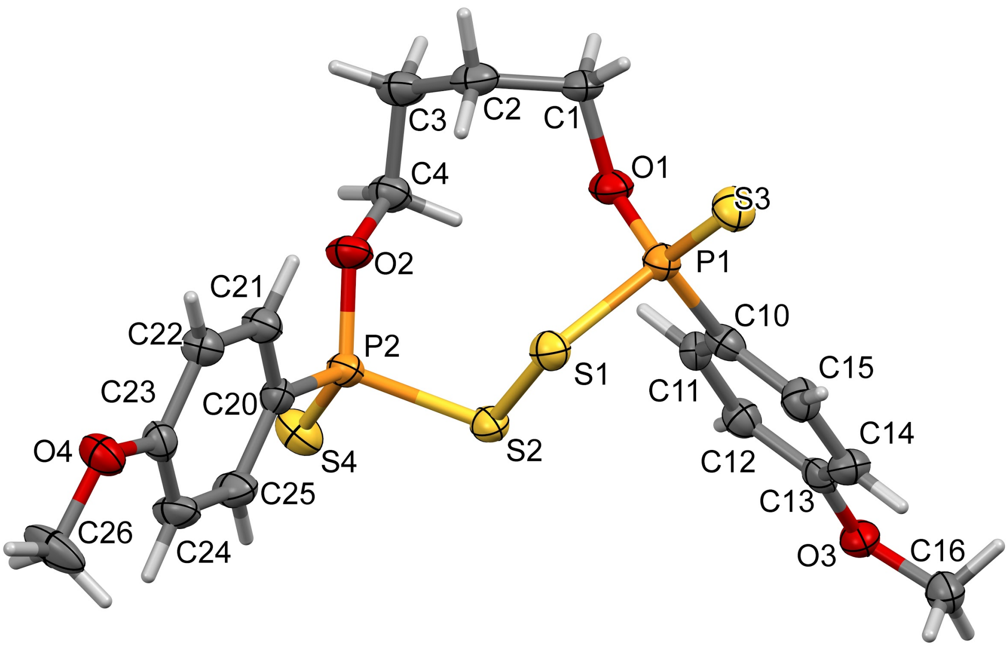

Figure S40. View of asymmetric unit of structure **2c** showing atom labelling scheme. Displacement ellipsoids drawn at 50% probability level.

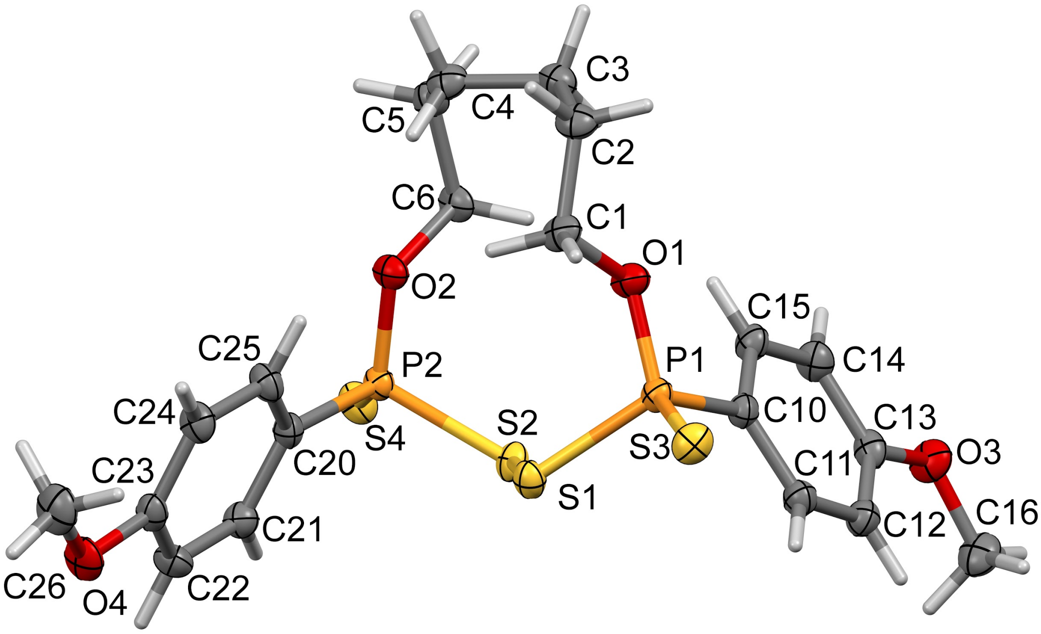

Figure S41. View of asymmetric unit of structure **2d_triclinic** showing atom labelling scheme. Displacement ellipsoids drawn at 50% probability level.

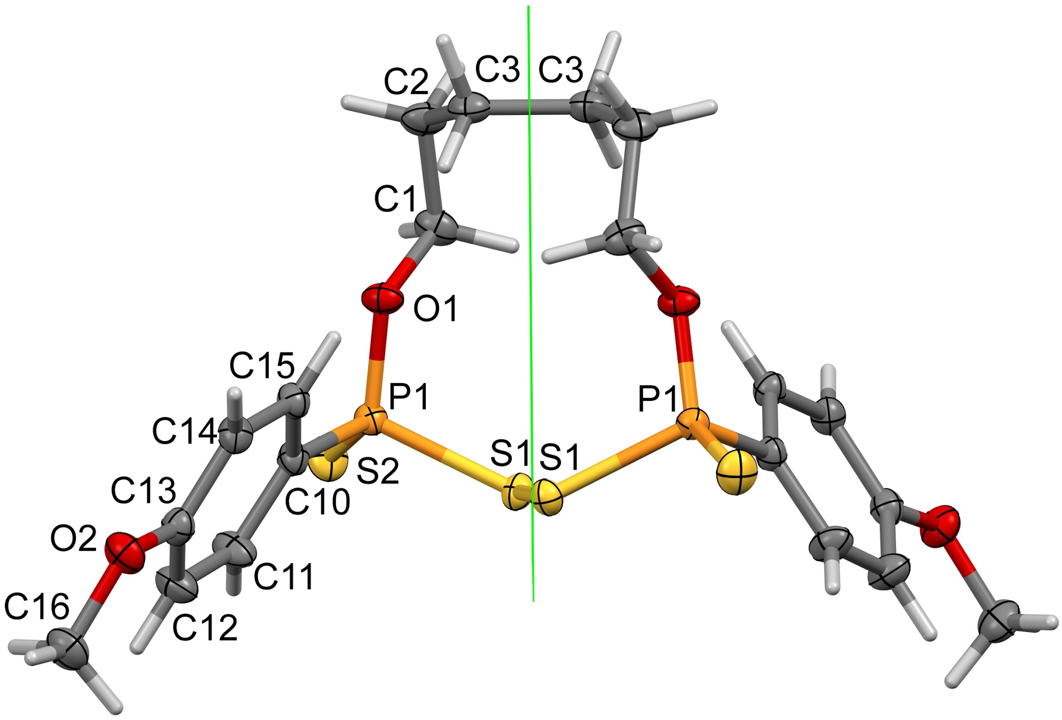

Figure S42. View of structure **2d_monoclinic** showing atom labelling scheme. Symmetry axis drawn as the green line, only three labels for symmetry equivalent atoms shown. Displacement ellipsoids drawn at 50% probability level.

All the compounds exhibit the *trans* (*anti*) conformation of the anisole residues in relation to the macrocycle and with both P=S groups directed outside the ring. The compounds crystallize in various space groups and with different molecular symmetry, which must be taken into account during comparison of geometry. Asymmetric unit of **2a** (with the $–CH_2$-CH_2- organic part of the macrocycle) contains half of the molecule since its symmetry is described by the C_2 point group (Schoenflies) with the two-fold axis passing through the centers of bonds S1—S1#1 and C1—C1#1 (#1 symmcode: 1+y, -1+x, -z). Asymmetric units of **2b**, **2b'** and **2d_triclinic** contain one molecule each. The monoclinic polymorph of **2d** again contains half of the molecule with a two-fold axis passing through bonds S1—S1#1 and C3—C3#1 (where #1 denotes: 1-x, y, ½ -z). Molecular symmetry is also described by the C_2 group.

Structures of disulfanes **3** have been also determined by X-Ray structural analyses in this study. Crystallographic data and refinement details for both conformers of **3a**, **3b** and **3d** are given in Table S2. Molecular views of the structures are presented in Figures S43-S48. In three cases i.e. for **3a_trans**, **3a_cis**, and **3b_cis** the asymmetric unit is composed of two molecules.

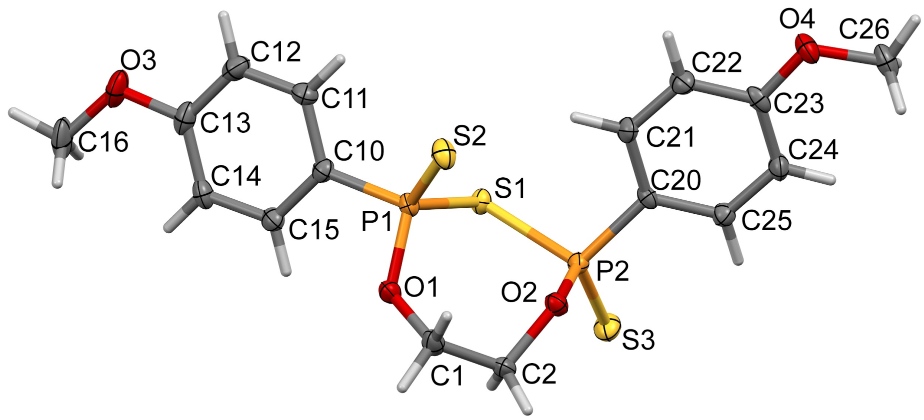

Figure S43. View of structure **3a_trans** showing atom labelling scheme. Only one molecule from the asymmetric unit is shown. Displacement ellipsoids drawn at 50% probability level.

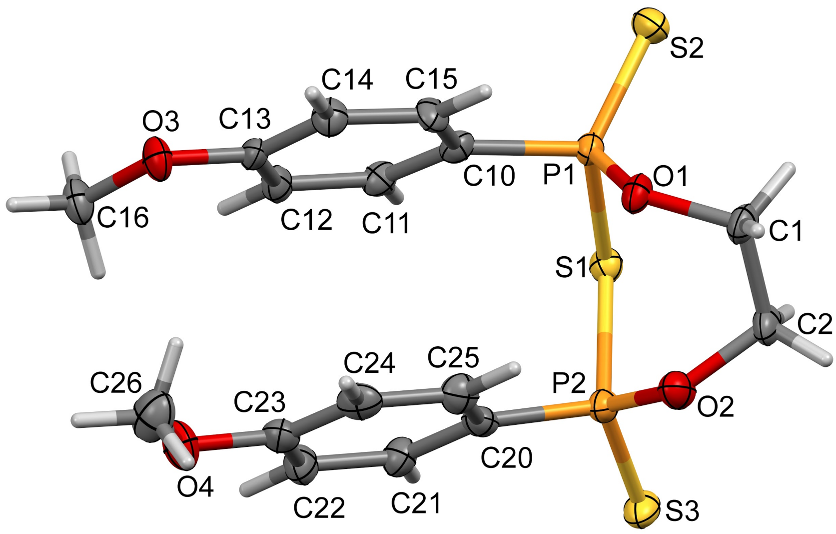

Figure S44. View of structure **3a_cis** showing atom labelling scheme. Only one molecule from the asymmetric unit is shown (out of two). Displacement ellipsoids drawn at 50% probability level.

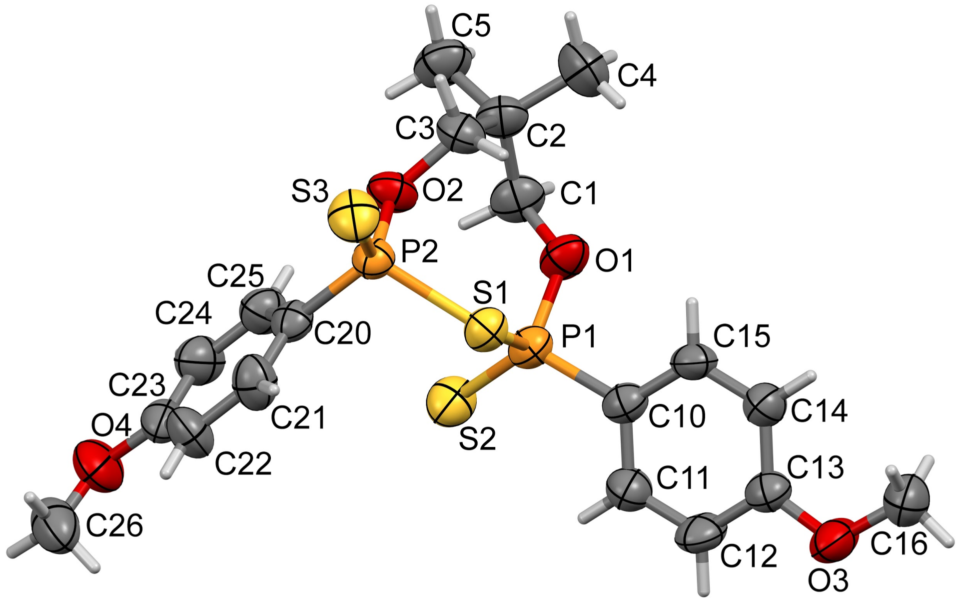

Figure S45. View of structure **3b_trans** showing atom labelling scheme. The asymmetric unit contains one molecule. Displacement ellipsoids drawn at 50% probability level.

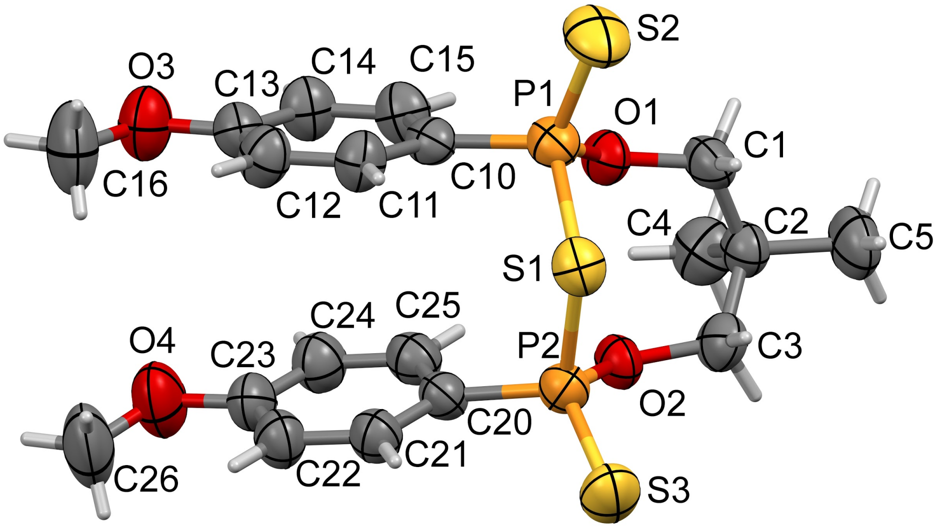

Figure S46. View of structure **3b_cis** showing atom labelling scheme. Only one molecule from the asymmetric unit is shown (out of two, Z' = 2). Displacement ellipsoids drawn at 50% probability level.

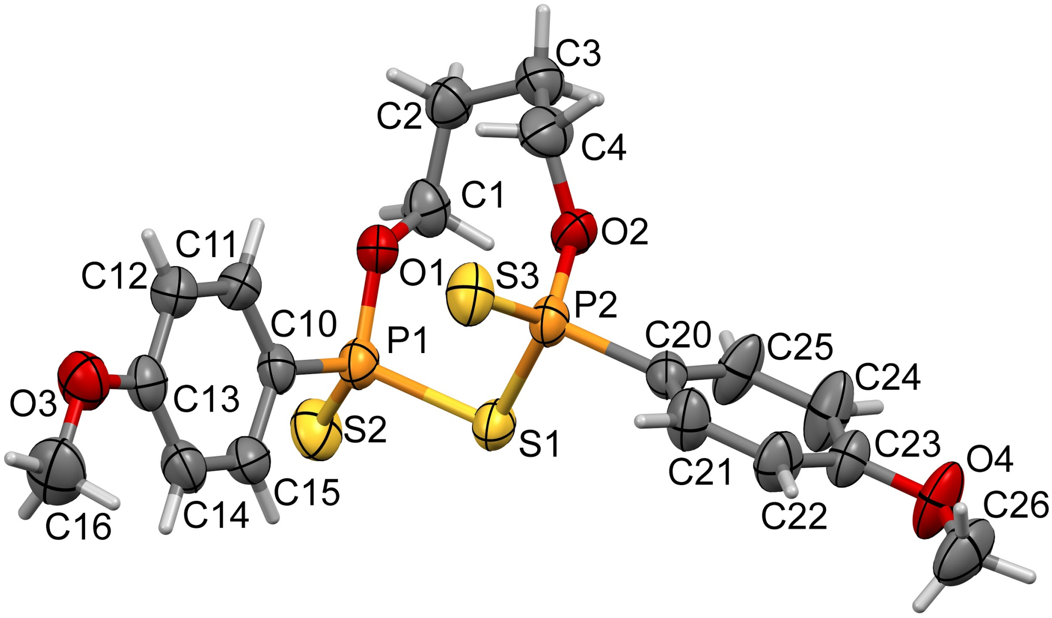

Figure S47. View of asymmetric unit of structure **3c_trans** showing atom labelling scheme. Displacement ellipsoids drawn at 50% probability level.

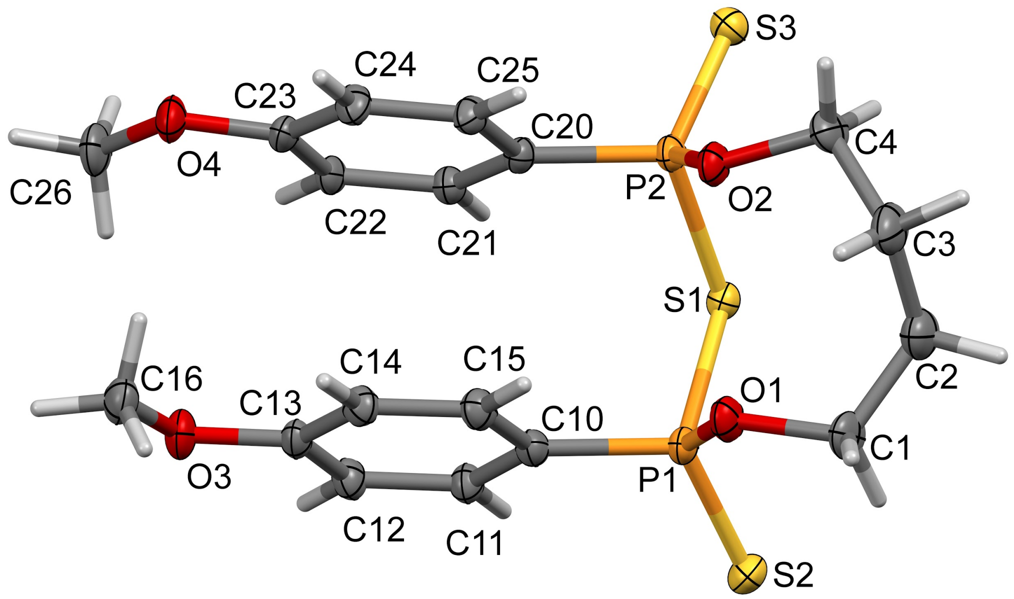

Figure S48. View of asymmetric unit of structure **3c_cis** showing atom labelling scheme. Displacement ellipsoids drawn at 50% probability level.

Ring conformations. Having the X-ray data we can analyse conformations of 8-, 9-, and 10- and 12-membered bis(anisylphosphonothioyl) disulfanes, for **2a**, **2b**, **2c** and **2d**, respectively. For definitions of conformations for large macrocycles see: ring puckering analysis [e.g. D. Cremer & J.A. Pople, J.Amer.Chem.Soc., 97, (1975), 1354-1358, D. Cremer, Acta Cryst. (1984). B40, 498-500, G.G. Evans & J.A. Boeyens, Acta Cryst. (1989), B45, 581-590].
A large interring P-S-S-P torsion angle, increasing with the ring size from *ca* 94° to *ca* 125°, is the most characteristic structural feature of cyclic disulfanes **2**.
Bonds and angles comparative study.

Related geometric parameters for all disulfanes **2** are gathered in Table S4.

Tables

Table S2. Details of the X-ray data collections and refinements for cyclic disulfanes **2a**-**d***

	2a	**2b**	**2b'**	**2c**	**2d_triclinic**	**2d_monoclinic**
Crystal data						
Chemical formula	$C_{16}H_{18}O_4P_2S_4$	$C_{19}H_{24}O_4P_2S_4$	$C_{20}H_{24}O_6P_2S_4$	$C_{18}H_{22}O_4P_2S_4$	$C_{20}H_{26}O_4P_2S_4$	$C_{20}H_{26}O_4P_2S_4$
M_r	464.48	506.56	550.57	492.53	520.59	520.59
Crystal system, space group	Tetragonal, $P4_32_12$	Monoclinic, $P2_1/c$	Triclinic, P-1	Monoclinic, $P2_1/c$	Triclinic, P-1	Monoclinic, $C2/c$
Temperature (K)	296	130	120	120	120	120
a, b, c (Å)	7.2415 (3), 7.2415 (3), 39.516 (2)	12.3171 (12), 9.1385 (5), 21.439 (2)	6.8942 (8), 9.3182 (11), 19.921 (3)	9.4262 (6), 13.3761 (8), 17.7998 (13)	10.4186 (13), 10.5778 (11), 12.5703 (15)	12.6554 (19), 8.5028 (9), 23.058 (4)
α, β, γ (°)	90, 90, 90	90, 96.512 (8), 90	95.844 (10), 90.407 (10), 93.486 (10)	90, 90.068 (7), 90	71.900 (9), 67.807 (9), 82.881 (9)	90, 101.230 (12), 90
V (Å^3)	2072.2 (2)	2397.6 (4)	1270.6 (3)	2244.3 (3)	1219.2 (3)	2433.7 (6)
Z	4	4	2	4	2	4
Radiation type	Mo *K*α	Mo *K*α	Mo *K*α	Mo *K*α	Mo *K*α	Mo *K*α
μ (mm^{-1})	0.63	0.55	0.53	0.59	0.55	0.55
Crystal size (mm)	0.44 × 0.42 × 0.03	0.34 × 0.03 × 0.02	0.35 × 0.29 × 0.17	0.21 × 0.20 × 0.14	0.31 × 0.15 × 0.05	0.34 × 0.15 × 0.11
Data collection						
Diffractometer	KM4CCD, Sapphire2	STOE *IPDS* 2T diffractometer	KM4CCD, Sapphire2	KM4CCD, Sapphire2	STOE *IPDS* 2T diffractometer	STOE *IPDS* 2T diffractometer
Absorption correction	Multi-scan	None	Multi-scan	Analytical	None	None
T_{min}, T_{max}	0.689, 0.98	–	0.891, 1	0.893, 0.929	–	–
No. Of measured, independent and observed [$I > 2\sigma(I)$] reflections	14211, 2019, 1839	9945, 4378, 4046	7730, 4687, 3746	9496, 4047, 3309	9505, 5339, 4702	8581, 3264, 2762
R_{int}	0.036	0.017	0.028	0.051	0.109	0.027
$(\sin \theta/\lambda)_{max}$ (Å^{-1})	0.617	0.608	0.604	0.606	0.647	0.686
Refinement						
$R[F^2 > 2\sigma(F^2)]$, $wR(F^2)$, $GooF$	0.038, 0.092, 1.09	0.025, 0.068, 1.07	0.054, 0.147, 1.05	0.082, 0.241, 1.05	0.068, 0.193, 1.07	0.027, 0.074, 1.05
No. Of reflections	2019	4378	4687	4047	5339	3264
No. Of parameters	120	266	289	256	273	137
H-atom treatment	parameters constrained	parameters constrained	parameters constrained	parameters constrained	parameters constrained	parameters constrained
Δ〉$_{max}$, Δ〉$_{min}$ (e Å^{-3})	0.33, -0.22	0.35, -0.22	1.37, -0.34	2.27, -0.84	0.82, -0.84	0.36, -0.27
Absolute structure	Refined as an inversion twin.	–	–	–	–	–
Abs. str. parameter	0.45 (17)	–	–	–	–	–
CCDC number	**719124**	**1560159**	**719125**	**1558043**	**1558050**	**1558049**

* structures of **2a** and **2c** were already published (W. Przychodzeń, J. Chojnacki, *Acta Cryst*., 2018, **E74**, 212–216)

Table S3. Details of the X-ray data collections and refinements for cyclic sulfanes **3**

	3a_trans	**3a_cis**	**3b_trans**	**3b_cis**	**3c_trans**	**3c_cis**
	Crystal data					
Chemical formula	$C_{16}H_{18}O_4P_2S_3$	$C_{16}H_{18}O_4P_2S_3$	$C_{19}H_{24}O_4P_2S_3$	$C_{19}H_{24}O_4P_2S_3$	$C_{18}H_{22}O_4P_2S_3$	$C_{18}H_{22}O_4P_2S_3$
M_r	432.42	432.42	474.5	474.5	460.47	460.47
Crystal system, space group	Monoclinic, $P2_1/c$	Orthorhombic, $Pna2_1$	Monoclinic, Pc	Monoclinic, $P2_1/n$	Triclinic, P-1	Triclinic, P-1
Temperature (K)	130	150	293	293	293	120
a, b, c (Å)	7.2217 (5), 15.7169 (6), 33.5977 (17)	20.284 (6), 21.511 (6), 8.717 (4)	14.6528 (5), 9.1347 (3), 17.8598 (6)	11.2880 (18), 18.3863 (13), 12.2511 (11)	8.5551 (6), 10.9717 (8), 13.0957 (10)	8.7882 (11), 8.8878 (10), 14.120 (2)
α, β, γ (°)	90, 92.598 (5), 90	90, 90, 90	90, 108.073 (4), 90	90, 112.627 (13), 90	113.352 (7), 104.434 (7), 93.127 (6)	73.295 (11), 75.044 (11), 81.888 (9)
V (Å^3)	3809.5 (4)	3803 (2)	2272.57 (14)	2346.9 (5)	1076.52 (15)	1017.8 (2)
Z	8	8	4	4	2	2
Radiation type	Mo $K\alpha$	Mo $K\alpha$	Mo $K\alpha$	Mo $K\alpha$	Mo $K\alpha$	Mo $K\alpha$
μ (mm^{-1})	0.58	0.58	0.49	0.47	0.51	0.54
Crystal size (mm)	0.29 × 0.05 × 0.02	0.21 × 0.08 × 0.07	0.29 × 0.17 × 0.11	0.13 × 0.04 × 0.02	0.41 × 0.26 × 0.02	0.44 × 0.23 × 0.11
Data collection						
Diffractometer	STOE *IPDS* 2T diffractometer	STOE *IPDS* 2T diffractometer	KM4CCD, Sapphire2	KM4CCD, Sapphire2	KM4CCD, Sapphire2	STOE *IPDS* 2T diffractometer
Absorption correction	Integration	None	Multi-scan	Multi-scan	Multi-scan	Integration
T_{min}, T_{max}	0.834, 0.973	-	0.852, 1	0.889, 1	0.551, 1	0.971, 0.992
No. of measured, independent and observed [$I > 2\sigma(I)$] reflections	15794, 7366, 5071	17031, 8098, 6283	15538, 7935, 6588	11898, 4297, 2318	6586, 3990, 2275	14738, 5492, 3596
R_{int}	0.057	0.052	0.036	0.061	0.092	0.064
$(\sin \theta/\lambda)_{max}$ (Å^{-1})	0.617	0.650	0.617	0.606	0.606	0.688
Refinement						
$R[F^2 > 2\sigma(F^2)]$, $wR(F^2)$, $GooF$	0.053, 0.127, 1.02	0.054, 0.129, 1.05	0.052, 0.133, 1.05	0.061, 0.173, 1.07	0.064, 0.18, 1.03	0.061, 0.173, 0.94
No. of reflections	7366	8098	7935	4297	3990	5492
No. of parameters	455	456	506	253	244	246
No. of restraints	0	1	2	0	0	0
H-atom treatment	parameters constrained	parameters constrained	parameters constrained	parameters constrained	parameters constrained	parameters constrained
$\Delta\rangle_{max}$, $\Delta\rangle_{min}$ (e Å^{-3})	0.62, -0.43	0.74, -0.36	0.55, -0.38	0.32, -0.45	0.51, -0.58	1.49, -0.66

Absolute structure	–	Refined as an inversion twin.	Refined as an inversion twin.	–	–	–
Absolute structure parameter	–	0.11 (13)	0.05 (12)	–	–	–
CCDC number	**1558051**	**1561560**	**944069**	**944068**	**1558052**	**1558054**

Table S4. Geometric parameters for cyclic disulfanes **2** and a reference, acyclic structure*

	2a	**2b**	**2b'**	**2c**	**2d_tri**	**2d_mono**	**ref [*Woollins*]**
independent molecules, Z'	½	1	1	1	1	½	2
Bond lengths, Å							
P1—S1	2.101(1)	2.1083(6)	2.118(1)	2.117(2)	2.111(1)	2.1088(7)	2.1153(6) and 2.1023(7)
P1=S3 (or P1=S2 *)	1.922(2)	1.9276(6)	1.936(1)	1.931(3)	1.9305(9)	1.9299(6)	1.9303(7) and 1.9305(8)
P2—S2	-	2.1085(6)	2.106(1)	2.090(3)	2.1043(9)	-	2.1090(7) and 2.1037(6)
P2=S4	-	1.9248(6)	1.946(1)	1.933(3)	1.9313(9)	-	1.9344(6) and 1.9295(7)
S1—S2 (S1—S1#1**)	2.068(2)	2.0704(6)	2.081(1)	2.074(3)	2.0705(9)	2.0759(5)	2.0850(8) and 2.0831(7)
P1—O1	1.584(2)	1.580(1)	1.602(2)	1.580(5)	1.586(2)	1.580(1)	1.583(1) and 1.582(1)
P2—O2	-	1.589(1)	1.602(2)	1.582(5)	1.590(2)	-	1.583(1) and 1.585(1)
P1—C10	1.787(3)	1.780(2)	1.794(4)	1.797(7)	1.780(2)	1.779(1)	1.780(2) and 1.779(2)
P2—C20	-	1.780(1)	1.795(3)	1.794(7)	1.780(3)	-	1.785(2) and 1.784(2)
valence angles, °							
S1—P1=S3 (S1—P1=S2 *)	104.43(6)	104.82(2)	102.41(5)	104.2(1)	103.16(4)	103.16(2)	103.17(3) and 103.78(3)
S2—P2=S4	-	104.84(2)	104.01(5)	103.0(1)	101.39(4)	-	104.50(3) and 102.64(3)
S1—P1—O1	106.96(9)	107.32(4)	107.75(9)	108.6(2)	108.65(8)	109.11(4)	105.66(5) and 106.62(5)
S2—P2—O2	-	106.89(4)	108.32(9)	108.2(2)	109.73(8)	-	107.34(5) and 105.87(5)
S1—P1—C10	109.6(1)	109.08(5)	108.2(1)	105.2(2)	107.11(9)	107.52(4)	110.47(6) and 108.96(6)
S2—P2—C20	-	109.95(5)	109.1(1)	109.4(2)	108.27(9)	-	109.55(6) and 111.20(6)
S3=P1—C10 (S2=P1—C10 *)	116.2(1)	115.95(5)	120.0(1)	118.5(2)	118.55(9)	118.84(5)	116.75(6) and 117.84(7)
S4=P2—C20	-	116.88(5)	117.1(1)	116.5(2)	118.41(9)	-	116.42(6) and 117.76(6)
P1—S1—S2 (P1-S1-S1#1*)	105.16(6)	103.57(2)	104.74(5)	103.1(1)	104.81(4)	105.53(2)	104.65(3) and 102.07(3)
P2—S2—S1	-	104.59(2)	103.23(5)	105.9(1)	107.23(4)	-	103.64(3) and 103.37(2)
Torsion angles, °							
S3=P1-S1-S2 S2=P1-S1-S1#1	164.53(6)	176.23(2)	178.39(5)	-171.0(1)	-163.94(4)	-161.12(2)	-171.21(3)and -170.28(3)
S1-S2-P2=S4	-	-179.55(2)	176.61(5)	174.9(1)	-166.26(4)	-	-173.52(3)and -172.28(3)

P1-S1-S2-P2 P1-S1-S1#1-P#1	-93.68(6)	-105.86(2)	106.77(5)	-112.9(1)	-114.35(4)	- 124.93(2)	-123.47(3) -126.30(3)
O1-P1-S1-S2 O1-P1-S1-S1#1	37.5(1)	50.55(5)	-56.7(1)	61.9(2)	70.67(9)	73.08(4)	-46.07(6) and -47.93(6)
S1-S2-P2-O2	-	54.46(5)	-57.1(1)	47.5(2)	68.77(9)	-	-44.43(6)and -47.83(5)
C10-P1-S1-S2 C10P1S1-S1#1*	-70.4(1)	-58.99(6)	50.7(1)	-45.7(3)	-38.1(1)	-34.74(5)	63.29(7) and 60.13(7)
C20-P2-S2-S1	-	-53.13(5)	50.9(1)	-60.6(3)	-41.0(1)	-	64.31(7) and 60.92(7)
C11-C10-P1-S3	178.1(3)	46.6(1)	154.0(3)	-153.5(5)	36.9(2)	28.8(1)	-12.3(2) and 148.6(1)
C21-C20-P2-S4	-	24.3(1)	-37.8(3)	-143.6(5)	35.8(2)	-	-17.6(2) and -34.3(2)
S3P1...O3CH3 S2 P1...O2CH3**	-178.2(3)	-129.2(1)	-33.9(3)	20.9(5)	42.0(2)	30.18(9)	-4.8(1) and -11.3(1)
S4P2...O4CH3	-	21.1(1)	139.4(2)	32.7(5)	-144.7(2)	-	140.6(1) and -38.4(1)

* structures of **2a** and **2c** were already published (W. Przychodzeń, J. Chojnacki, *Acta Cryst*., 2018, **E74**, 212–216)
** for Z'= ½, #1 for **2a**: 1+*y*, -1+*x*, -*z*; #1 for **2d**: 1-*x*, *y*, ½ -*z* (both are 2-fold rotations)

Table S5. Geometric parameters for cyclic sulfanes **3**

	Cis-3a	Trans-3a	Cis-3b	Trans-3b	Cis-3c	Trans-3c
independent molecules, Z'	2	2	1	2	1	1
Bond lengths, Å						
P1=S2	1.922(2)	1.923(1)	1.926(2)	1.924(3)	1.924(1)	1.927(2)
P2=S3	1.923(3)	1.931(1)	1.920(2)	1.917(3)	1.938(1)	1.918(2)
P3=S5	1.921(3)	1.924(1)	-	1.911(3)	-	-
P4=S6	1.926(2)	1.931(1)		1.921(2)		
P1—S1	2.101(3)	2.124(1)	2.103(2)	2.129(3)	2.130(1) 2.103(1)	2.113(3)
P2—S1	2.110(2)	2.120(1)	2.131(2)	2.118(3)		2.129(2)
P3—S4	2.111(2)	2.121(1)	-	2.140(2)	-	-
P4—S4	2.099(3)	2.117(1)		2.105(2)		
P1—O1	1.587(4)	1.588(3)	1.578(3)	1.585(5)	1.585(3)	1.586(4)
P2—O2	1.593(5)	1.589(2)	1.571(3)	1.596(5)	1.584(3)	1.588(4)
P3—O5	1.586(5)	1.594(3)	-	1.582(6)	-	-
P4—O6	1.585(4)	1.592(2)		1.593(5)		
P1—C10	1.788(7)	1.783(3)	1.782(5)	1.792(7)	1.777(3)	1.785(5)
P2—C20	1.782(7)	1.788(3)	1.779(5)	1.780(6)	1.779(3)	1.802(6)
P3—C30	1.771(7)	1.783(3)	-	1.794(7)	-	-
P4—C40	1.794(7)	1.780(3)				
valence angles, °						

S1P1=S2 S1P2=S3	107.3(1) 105.1(1)	116.79(6) 108.44(5)	106.05(8)	114.3(1) 105.0(1)	105.45(5) 105.77(5)	107.64(9) 116.8(1)
S4P3=S5 S4P4=S6	105.7(1) 106.7(1)	115.80(6) 108.16(6)	-	115.6(1) 105.8(1)	-	-
O1P1=S2 O2P2=S3	117.3(2) 117.4(2)	116.3(1) 116.8(1)	116.8(1) 119.0(1)	117.2(2) 117.6(2)	118.3(1) 116.8(1)	117.1(2) 117.5(2)
O5P3=S5 O6P4=S6	117.7(2) 117.3(2)	116.6(1) 116.0(1)	-	117.1(2) 117.3(2)	-	-
O1P1—S1 O2P2—S1	106.3(2) 106.1(2)	103.4(1) 105.4(1)	106.3(1) 105.6(1)	104.7(2) 104.2(2)	106.6(1) 107.4(1)	105.5(2) 100.8(2)
O5P3—S4 O6P4—S4	106.3(2) 106.0(2)	104.1(1) 105.7(1)	-	104.3(2) 105.0(2)	-	-
O1P1C10 O2P2C20	98.3(3) 102.5(3)	100.9(1) 101.2(1)	101.6(2) 101.9(2)	102.6(2) 102.3(2)	102.7(1) 101.5(1)	101.2(2) 103.5(2)
O5P3C30 O6P4C40	102.2(3) 98.9(3)	100.0(1) 100.9(1)	-	1.794(7) 1.786(8)	-	-
P1-S1-P2	105.73(9)	105.28(5)	108.70(8)	106.4(1)	108.77(5)	103.00(9)
P3-S4-P4	105.66(9)	104.19(5)	-	105.1(1)	-	-
P1-O1-C1 P2-O2-C2/N*	125.1(4) 122.5(4)	123.0(2) 123.1(2)	120.1(3) 121.9(3)	124.1(5) 120.3(4)	121.0(2) 122.1(2)	120.9(3) 125.6(3)
P3-O5-C50 P4-O6-C51/M*	121.8(4) 124.6(4)	123.2(2) 125.0(2)	-	125.2(5) 118.1(4)	-	-
(*) N and M denote the terminal C atom number in the macrocyclic ring						
Torsion angles, °						
S2=P1-S1-P2 P1-S1-P2=S3	154.9(1) -170.5(1)	65.47(7) 137.14(6)	-166.95(8) 170.53(8)	-57.1(1) -163.3(1)	-174.57(5) 172.32(5)	164.85(9) 58.2(1)
S5=P3-S4-P4 P3-S4-P4=S6	170.6(1) -155.2(1)	-69.34(7) -131.90(6)	-	57.2(1) 163.5(1)	-	-
C11C10P1=S2 C21C20P2=S3	94.8(6) -38.6(6)	31.4(3) 153.6(3)	-73.6(4) 36.3(4)	-19.5(7) -45.0(7)	-41.9(3) 74.1(3)	-121.1(4) 17.8(5)
C31C30P3=S5	42.4(6) -94.2(6)	-40.2(3) -155.8(3)	-	26.3(7) 59.0(7)	-	-

C41C40P4=S6						
S2P1...P2S3	-23.6(2)	174.21(7)	6.0(2)	155.4(2)	-3.6(1)	-155.7(1)
S5P3...P4S6	23.0(2)	-172.00(7)	-	-156.5(2)	-	-
S2P1...O3CH$_3$ S3P2...O4CH$_3$	100.8(4) 147.8(5)	-142.4(3) -22.7(3)	-77.4(4) 29.7(4)	162.4(5) -41.7(6)	139.5(2) 78.0(2)	62.1(4) 21.0(5)
S5P3...O7CH$_3$ S6P4...O8CH$_3$	-143.1(5) -99.8(5)	130.4(3) -155.7(2)	-	-162.6(5) -102.7(6)	-	-

Table S6. Hydrogen-bond geometry (Å,°) for investigated cyclic disulfanes **2**.

D—H···*A*	*D*—H	H···*A*	*D*···*A*	*D*—H···*A*
Comp **2b**				
C12—H12···O4^{i}	0.95	2.49	3.4346 (18)	171
C26—H26*C*···S4^{ii}	0.98	2.79	3.7602 (16)	169
Symmetry codes: (i) *x*, -*y*+5/2, *z*-1/2; (ii) *x*, -*y*+3/2, *z*+1/2				
Comp **2b'**				
C2—H2···S4^{i}	1.00	2.93	3.783 (4)	144
C6—H6*C*···O3^{i}	0.98	2.66	3.450 (6)	138
C6—H6A···S2^{ii}	0.98	3.02	3.671 (5)	125
C15—H15···S3^{iii}	0.95	2.94	3.773 (4)	148
Symmetry codes: (i) *x*-1, *y*, *z*; (ii) *x*-1, *y*+1, *z*; (iii) -*x*+1, -*y*+1, -*z*				

Comp *syn*-**2d** mono				
C16—H16*B*···S2^{i}	0.98	3.03	3.9768 (16)	163
C16—H16*C*···O2^{ii}	0.98	2.53	3.3626 (18)	143
Symmetry codes: (i) -x+1, -y, -z+1; (ii) -x+2, -y, -z+1				
Comp *anti*-**2d** tri				
C15—H15···S4^{i}	0.95	2.97	3.684 (3)	133
C16—H16*A*···S4^{ii}	0.98	2.86	3.652 (3)	138
C16—H16*C*···S3^{iii}	0.98	3.00	3.827 (3)	143
C21—H21···S2^{iv}	0.95	2.95	3.617 (3)	129
C25—H25···S3^{v}	0.95	2.97	3.672 (3)	131
Symmetry codes: (i) -x+1, -y, -z+1; (ii) x, y-1, z; (iii) -x+2, -y-1, -z+1; (iv) -x+2, -y, -z+1; (v) -x+2, -y, -z.				

Table S7. Hydrogen-bond geometry (Å, °) for investigated sulfides **3**

D—H···*A*	*D*—H	H···*A*	*D*···*A*	*D*—H···*A*
Comp cis-**3a**				
C11—H11···S1	0.95	2.87	3.333 (6)	111
C15—H15···S3^{i}	0.95	3.00	3.871 (7)	153

C16—H16A···S3^{ii}	0.98	2.84	3.751 (7)	154
C16—H16B···S6^{iii}	0.98	3.02	3.675 (8)	126
C16—H16C···S4^{iv}	0.98	2.90	3.533 (8)	123
C36—H36A···S2^{ii}	0.98	3.01	3.754 (9)	133
C41—H41···S4	0.95	2.95	3.405 (6)	111
C42—H42···S2^{v}	0.95	3.02	3.931 (7)	161
C46—H46B···S1^{vi}	0.98	3.00	3.601 (8)	121
C52—H52B···O2^{i}	0.99	2.52	3.464 (8)	159
Symmetry codes: (i) x, y, z-1; (ii) -x+3/2, y+1/2, z-1/2; (iii) x-1/2, -y+3/2, z+1; (iv) x-1/2, -y+3/2, z; (v) x+1/2, -y+3/2, z; (vi) x+1/2, -y+3/2, z-1.				
Comp trans-**3a**				
C2—H2A···S6^{i}	0.99	2.88	3.622 (3)	132
C16—H16A···S2^{ii}	0.98	2.91	3.534 (5)	123
C21—H21···S2	0.95	2.80	3.614 (4)	144
C22—H22···O7^{iii}	0.95	2.55	3.457 (4)	160
C32—H32···S2^{ii}	0.95	2.91	3.721 (4)	144
C36—H36A···S5^{iv}	0.98	2.94	3.590 (4)	125
C41—H41···S5	0.95	2.91	3.718 (4)	143

C45—H45···O8^{v}	0.95	2.65	3.584 (4)	167
Symmetry codes: (i) -x, -y+2, -z; (ii) -x, y+1/2, -z+1/2; (iii) -x, y-1/2, -z+1/2; (iv) -x-1, y-1/2, -z+1/2; (v) -x, -y+3, -z.				
Comp cis-**3b**				
C2—H2···S1^{i}	0.93	2.75	3.460 (5)	134
C5—H5···S2^{ii}	0.93	2.89	3.790 (5)	162
C7—H7*A*···S2^{iii}	0.96	2.88	3.828 (7)	171
C14—H14*A*···S3^{iii}	0.96	3.01	3.881 (7)	151
Symmetry codes: (i) x+1/2, -y+1/2, z+1/2; (ii) -x+2, -y, -z; (iii) x+1, y, z.				
Comp trans-**3b**				
C16—H16*C*···S6^{i}	0.96	2.86	3.487 (9)	124
C26—H26*C*···S2^{ii}	0.96	2.74	3.674 (10)	166
C41—H41···O7^{iii}	0.93	2.54	3.389 (9)	153
C46—H46*A*···O3^{iv}	0.96	2.65	3.554 (11)	157
Symmetry codes: (i) x, -y+2, z+1/2; (ii) x, -y+1, z-1/2; (iii) x, -y+3, z-1/2; (iv) x+1, -y+2, z-1/2.				
Comp cis-**3c**				
C1—H1A···S2	0.99	2.84	3.408 (4)	117
C2—H2A···S1	0.99	2.95	3.660 (4)	130
C12—H12···S1^{i}	0.95	3.02	3.759 (3)	136

C14—H14···S3^{ii}	0.95	2.96	3.907 (3)	171
C16—H16A···S2^{iii}	0.98	2.91	3.742 (3)	143
C16—H16C···S1^{ii}	0.98	2.99	3.951 (4)	168
C24—H24···S3^{iv}	0.95	2.99	3.875 (3)	156
Symmetry codes: (i) -x+2, -y+1, -z; (ii) x+1, y, z; (iii) x+1, y-1, z; (iv) -x+2, -y, -z+1.				
Comp trans-**3c**				
C21—H21···S3	0.93	2.99	3.448 (6)	112
C21—H21···S3^{i}	0.93	3.09	3.952 (6)	156
C26—H26B···O3^{i}	0.96	2.56	3.462 (8)	156
Symmetry code: (i) -x+1, -y, -z.				

Table S8. Transannular hydrogens and transannular H-H repulsive and H-S attractive interactions taken from X-Ray structures and from calculated structures (in brackets) of **2** and **3**

Compd	transannular hydrogens	repulsive interaction	distance	transannular CH...S interaction /**hydrogen bond***	distance
trans-**2a**	-	-	-	-	-
(*trans*-**2a**)	-	-	-	-	-
(*cis*-**2a**)	-	-	-	-	-
trans-**2b**	C1H, C3H	-	-	C1H...S1 C3H...S2	3.109 3.109
(*trans*-**2b**)	C1H, C3H	-	-	C1H...S1 C3H...S2	3.032 3.057
(*cis*-**2b**)	C1H, C3H	-	-	C1H...S1 C3H...S2	3.108 3.070
trans-**2b'**	C1H, C3H	-	-	C1H...S1 C3H...S2	3.038 3.046
trans-**2c**	C1H, C3H	-	-	C1H...S1 C3H...S2	3.171 3.222
(*trans*-**2c)**	C1H, C3H	-	-	C1H...S1 C3H...S2	3.101 3.321
(*cis*-**2c**)	C1H, C3H	-	-	C1H...S1 C3H...S2	3.170 3.222
trans-**2d**	C1H, C4H, C3H, C6H	C1H...HC4 C3H...HC6	2.221 2.181	C1H...S1 C6H...S2	3.292 3.296
(*trans*-**2d**)	C1H, C4H, C3H, C6H	C1H...HC4 C3H...HC6	2.184 2.182	C1H...S1 C6H...S2	3.374 3.460
(*cis*-**2d**)	C1H, C4H, C3H, C6H	C1H...HC4 C3H...HC6	2.182 2.159	C1H...S1 C6H...S2	3.364 3.357
cis-**3a**	C1H	-	-	**C1H...S**	**2.767-2.786**
(*cis*-**3a**)	C1H		-	**C1H...S**	**2.739**
trans-**3a**	C1H, C3H	-	-	C1H...S	3.387
(*trans*-**3a**)	C1H, C3H	-	-	C1H...S	3.679
cis-**3b**	C1H, C3H	-	-	C1H...S C3H...S	3.082 3.044
(*cis*-**3b**)	C1H, C3H	-	-	C1H...S C3H...S	3.120 3.069
trans-**3b**	C1H	-	-	**C1H...S**	**2.838**
(*trans*-**3b**)	C1H	-	-	**C1H...S**	**2.873**

cis-**3c**	C2H, C3H	-	-	C3H...S	2.946
(*cis*-**3c**)	C2H, C3H	-	-	C3H...S	2.951
trans-**3c**	C1H, C4H	-	-	C1H...S	3.190
(*trans*-**3c**)	C1H, C4H	-	-	C1H...S	3.195

(*) Interactions in which the CH...S distance is smaller than the sum of the van der Waals radii (<2.9 A) are defined as hydrogen bonds and listed in bold

Calculations

The molecular structure of disulfanes **2** and sulfanes **3** was optimized with the density functional theory at MN12SX/6-311G* level using Gaussian 09 [2]. Solvent effects of dichloroethane were included using PCM continuum model. The optimized geometries were used to calculate the NMR parameters.

Dipole moments (debye) computed for molecules **3**

[2] M. J. Frisch, G. W. Trucks, H. B. Schlegel, G. E. Scuseria, M. A. Robb, J. R. Cheeseman, G. Scalmani, V. Barone, G. A. Petersson, H. Nakatsuji, X. Li, M. Caricato, A. Marenich, J. Bloino, B. G. Janesko, R. Gomperts, B. Mennucci, H. P. Hratchian, J. V. Ortiz, A. F. Izmaylov, J. L. Sonnenberg, D. Williams-Young, F. Ding, F. Lipparini, F. Egidi, J. Goings, B. Peng, A. Petrone, T. Henderson, D. Ranasinghe, V. G. Zakrzewski, J. Gao, N. Rega, G. Zheng, W. Liang, M. Hada, M. Ehara, K. Toyota, R. Fukuda, J. Hasegawa, M. Ishida, T. Nakajima, Y. Honda, O. Kitao, H. Nakai, T. Vreven, K. Throssell, J. A. Montgomery, Jr., J. E. Peralta, F. Ogliaro, M. Bearpark, J. J. Heyd, E. Brothers, K. N. Kudin, V. N. Staroverov, T. Keith, R. Kobayashi, J. Normand, K. Raghavachari, A. Rendell, J. C. Burant, S. S. Iyengar, J. Tomasi, M. Cossi, J. M. Millam, M. Klene, C. Adamo, R. Cammi, J. W. Ochterski, R. L. Martin, K. Morokuma, O. Farkas, J. B. Foresman, and D. J. Fox, Gaussian, Inc., Wallingford CT, 2016.

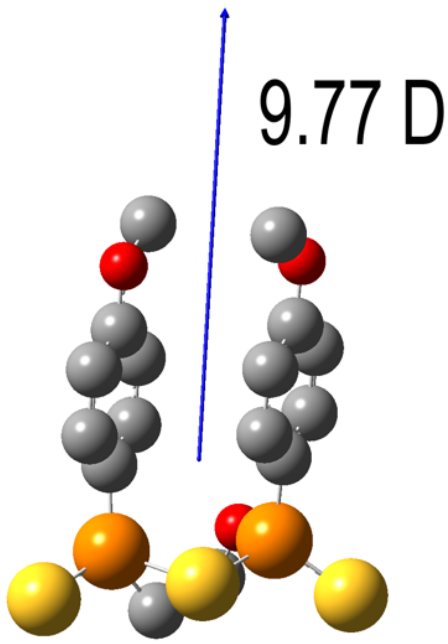

Figure S49. Dipole moment and its orientation for *cis*-**3a**

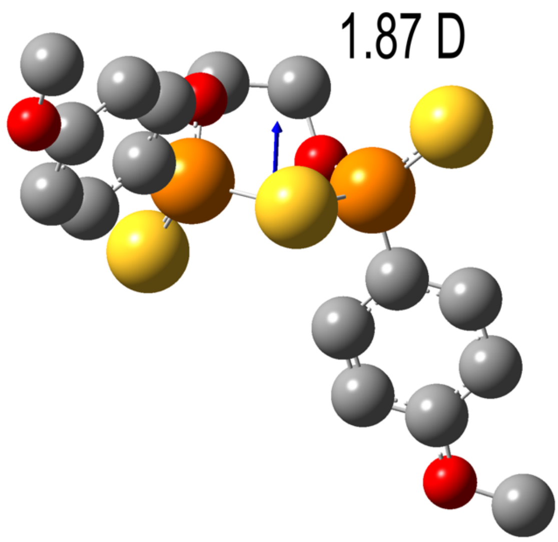

Figure S50. Dipole moment and its orientation for *trans*-**3a**

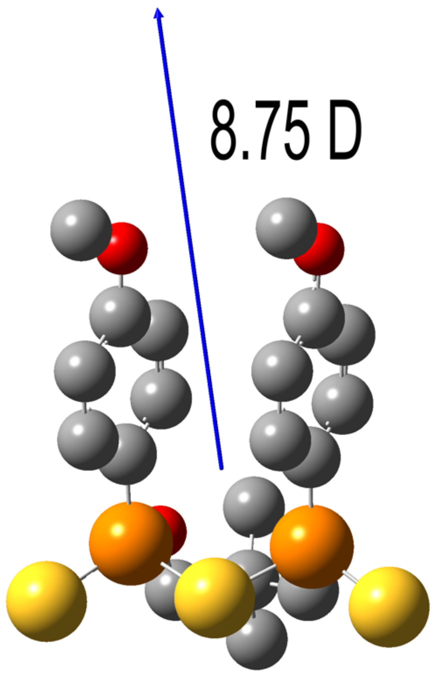

Figure S51. Dipole moment and its orientation for *cis*-**3b**

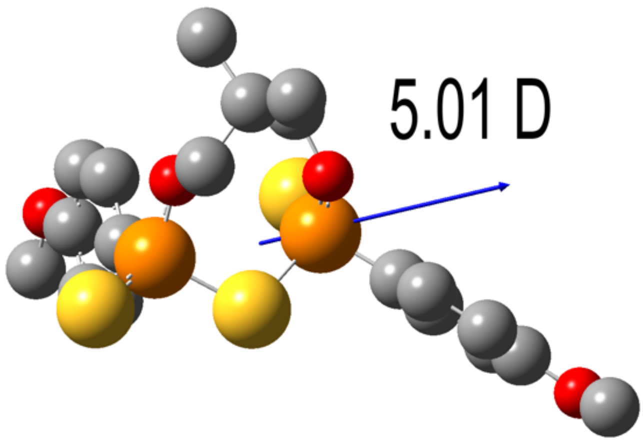

Figure S52. Dipole moment and its orientation for *trans*-**3b**

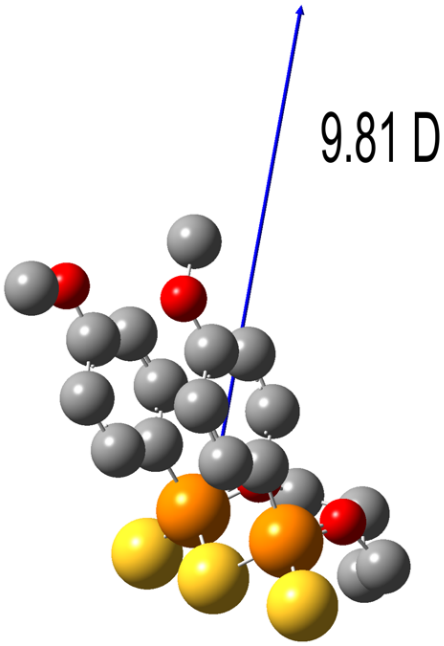

Figure S53. Dipole moment and its orientation for *cis*-**3c**

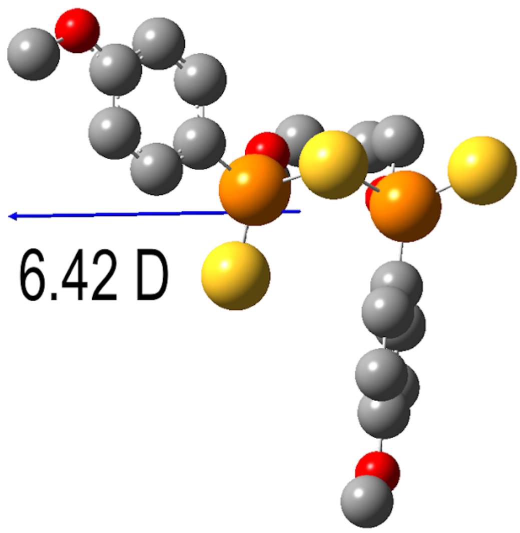

Figure S54. Dipole moment and its orientation for *trans*-**3c**